# Diffusional Transformations in Solids

# Contents

- Nucleation in solids
  - Homogeneous
  - Heterogeneous
- Overall Transformation Kinetics – TTT Diagrams
- Precipitation in Age Hardening Alloys
- Cellular Precipitation
- Eutectoid Decomposition
- Massive Transformations
- Ordering Transformations.

# Diffusional transformation in solids

- Conversion of single phase region to one or more stable phases with respect to temperature
  - Precipitation reactions
  - Eutectoid transformations
  - Ordering reactions
  - Massive transformations
  - Polymorphic changes

# Precipitation reactions

$$\alpha' \rightarrow \alpha + \beta$$

α‘ – metastable supersaturated solid solution
α – more stable solid solution
β - stable or metastable solid solution

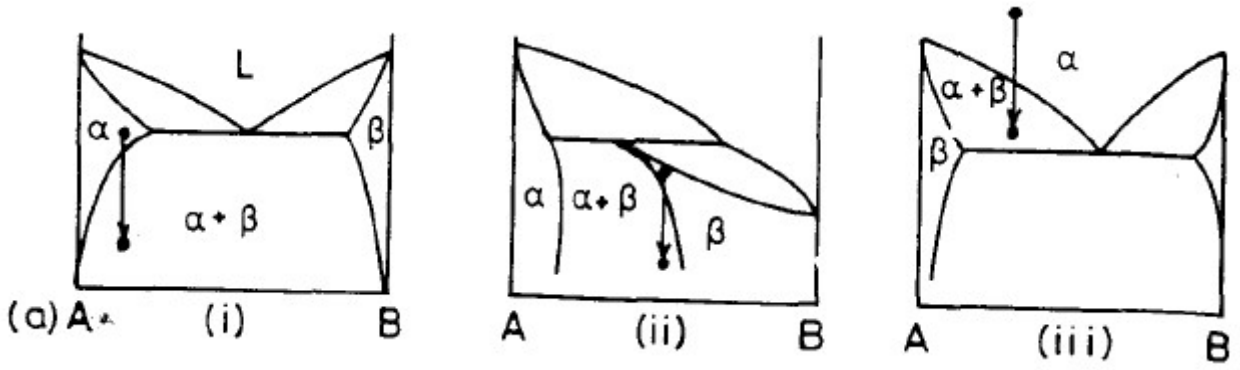

## Eutectoid Transformation

$$\gamma \rightarrow \alpha + \beta$$

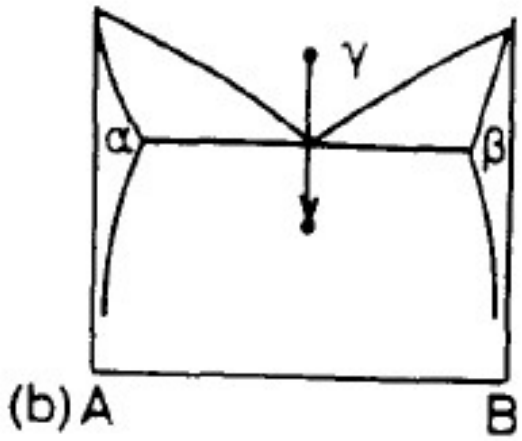


## Ordering Reactions

$$\alpha(disordered) \rightarrow \alpha'(ordered)$$

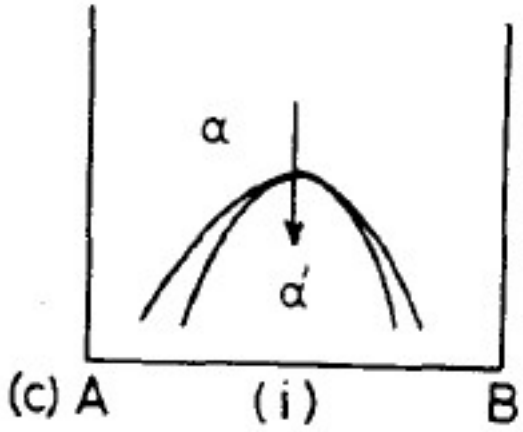


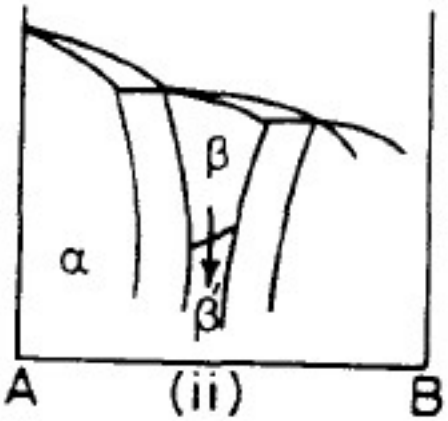

## Massive Transformation

$$\beta \rightarrow \alpha$$

Original phase decomposes into one more new phases

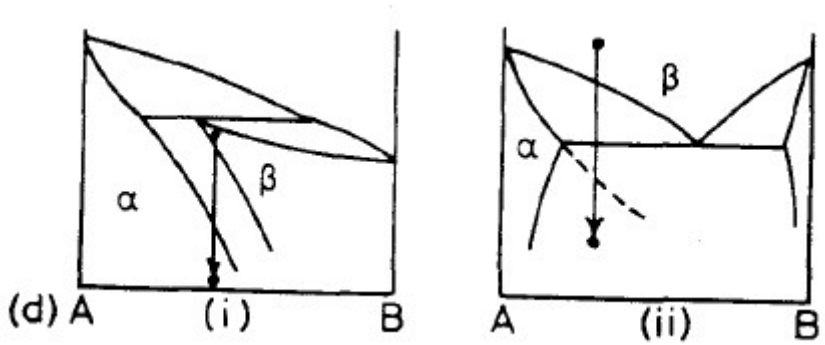


## Polymorphic changes

$$\alpha - Fe \leftrightarrow \gamma - Fe$$

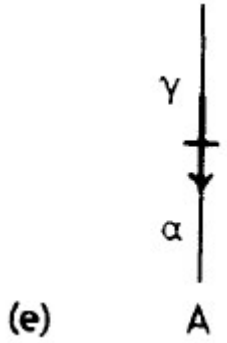

# Homogeneous Nucleation in Solids

Consider the precipitation reaction,

$$\alpha' \rightarrow \alpha + \beta$$

When temperature decreases, α/β interface created similar to L→ S transformation.

The free energy change associated with the reaction are,

$$\Delta G = -V\Delta G_V + A\gamma + V\Delta G_S$$

$\Delta G_V$-free energy reduction due to formation of β

V- volume of β phase formed

γ – interfacial energy of α and β

A – interface area

$\Delta G_S$- misfit strain energy per unit volume of β

$$\Delta G = -V\Delta G_V + A\gamma + V\Delta G_S$$

$$\Delta G = -\frac{4}{3}\pi r^3(\Delta G_V - \Delta G_S) + 4\pi r^2\gamma$$

The critical nucleus and Gibbs energy are,

$$r^* = \frac{2\gamma}{(\Delta G_V - \Delta G_S)}$$

$$\Delta G^* = \frac{16\pi\gamma^3}{3(\Delta G_V - \Delta G_S)^2}$$

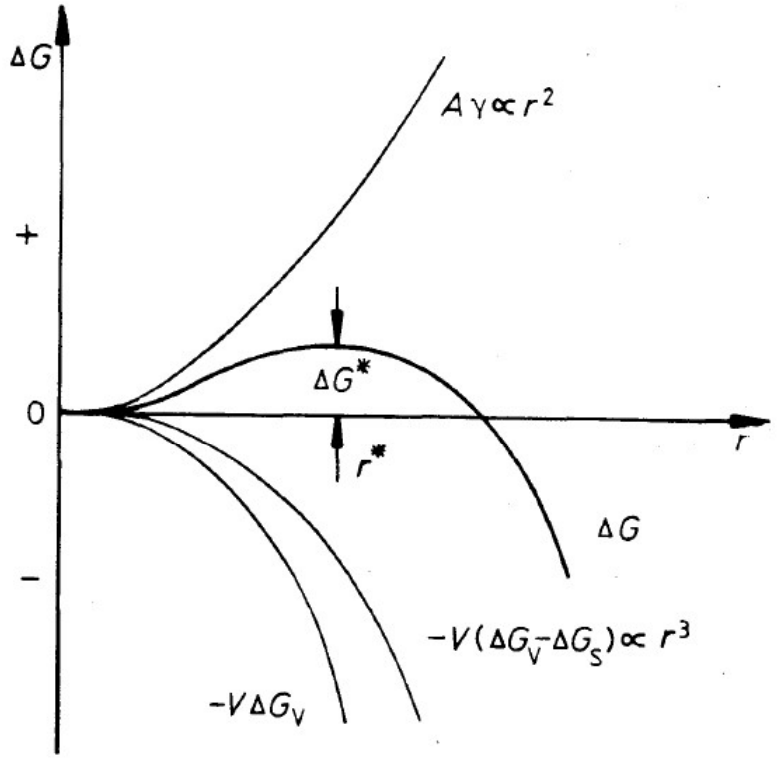


Misfit energy reduced the chemical driving force $\Delta G_v$

Concentration of critical sized nuclei C* is,

$$C^* = C_0 \exp(-\Delta G^* / kT)$$

$C_0$- number of atoms per unit volume.

The homogenous nucleation rate is,

$$N_{\text{hom}} = fC^*$$

*f* – rate of supercritical nucleus per second

The nucleation rate is,

$$N_{\text{hom}} = \omega C_0 \exp\left(-\frac{\Delta G_m}{kT}\right)\exp\left(-\frac{\Delta G^*}{kT}\right)$$

*ΔG**- strongly temperature dependent

The total free energy of the system will decreases by $\Delta G_1$ (at point P) is,

$$\Delta G_1 = \mu_A^\alpha X_A^\beta + \mu_B^\alpha X_B^\beta \quad \text{(per mol } \beta \text{ removed)}$$

The total free energy of the system will increase by an amount ( at point Q),

$$\Delta G_2 = \mu_A^\beta X_A^\beta + \mu_B^\beta X_B^\beta \quad \text{(per mol } \beta \text{ formed)}$$

Therefore, the driving force for nucleation,

$$\Delta G_n = \Delta G_2 - \Delta G_1 \quad \text{per mol of } \beta$$

The volume free energy decreases associated with the nucleation event is,

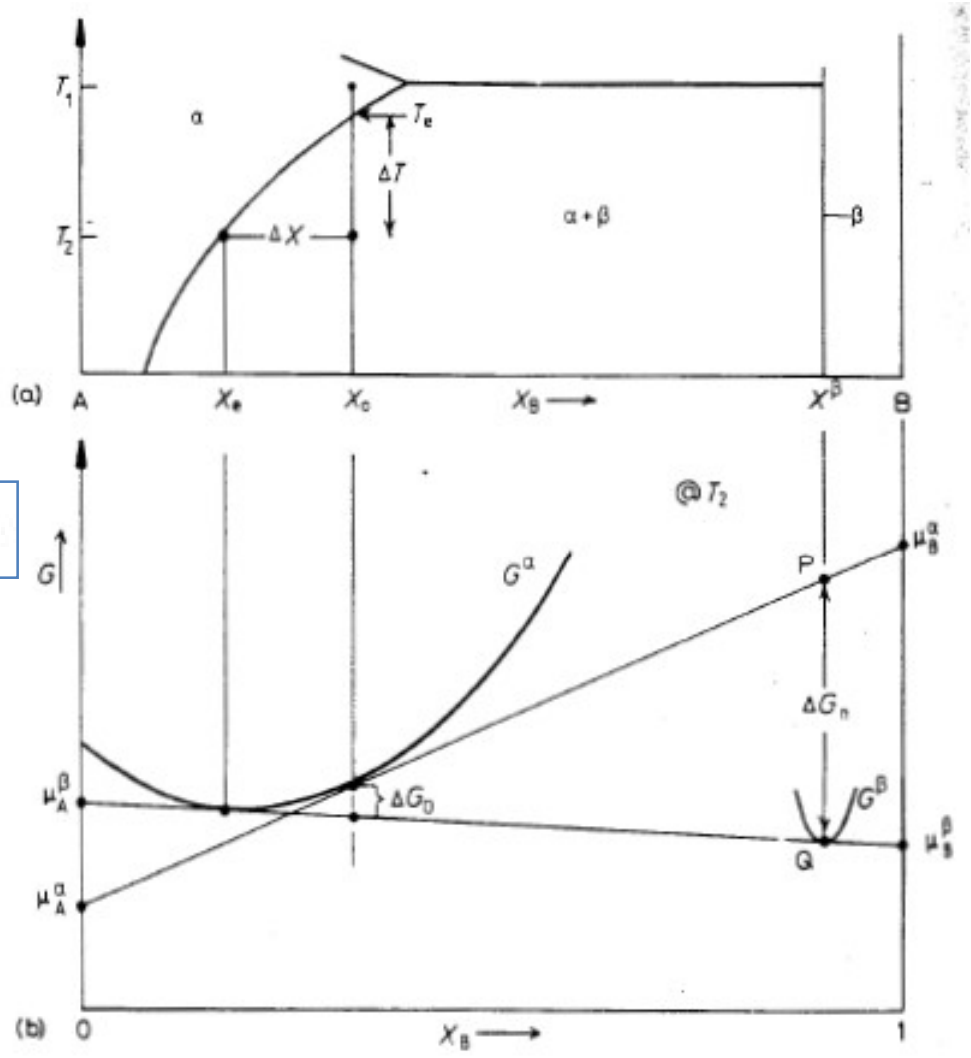


$$\Delta G_v = \frac{\Delta G_n}{V_m} \quad \text{per unit volume of } \beta$$

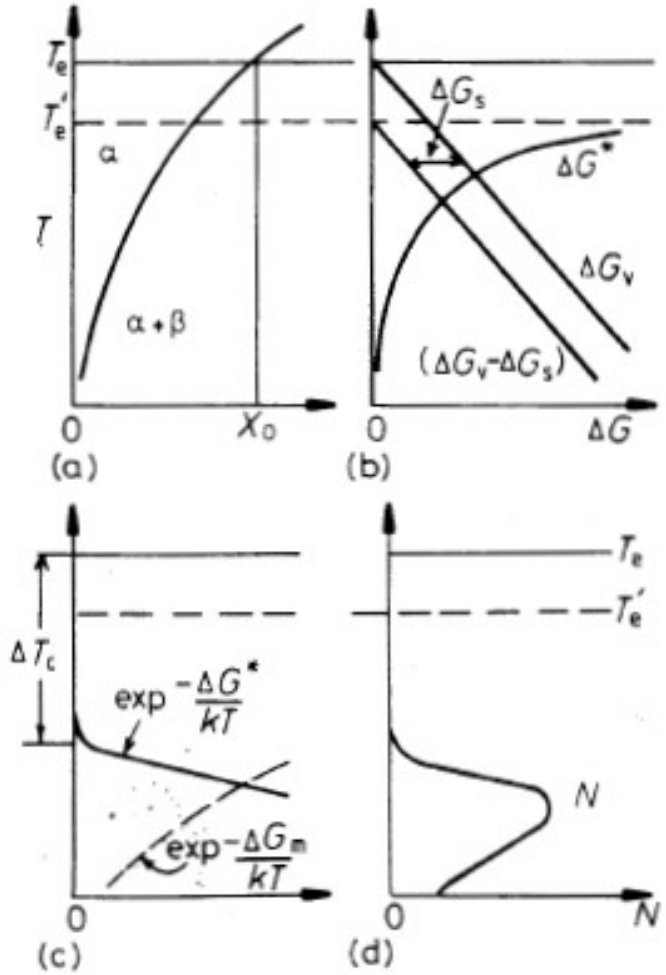


a) The phase diagram b) the effective driving force ($\Delta G_V$-$\Delta G_S$) and resultant energy barrier ΔG* c) the two exponential terms that determine N as shown d)

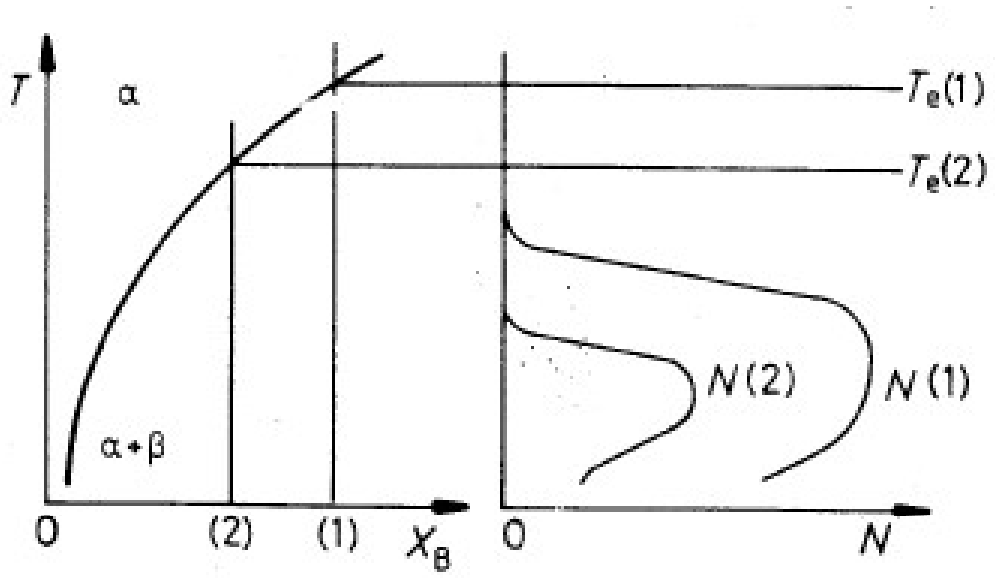


The effective alloy composition on the nucleation rate.

The nucleation rate in alloy 2 is always less than in alloy 1.

# Heterogeneous Nucleation

- Suitable nucleation sites are non-equilibrium defects such as excess vacancies, dislocations, grain boundaries, stacking faults, inclusions and free surfaces.
- Creation of a nucleus results in the destruction of a defect which reduces the activation energy barrier (corresponding Gibbs energy is $\Delta G_d$)
- The change in Gibbs energy due to heterogeneous nucleation is,

$$\Delta G = -V(\Delta G_V - \Delta G_S) + A\gamma - \Delta G_d$$

**Nucleation in Grain boundaries:**

Consider misfit strain energy is negligible. The optimum shape for incoherent grain boundary nucleus is two abutted special cap with θ is

$$\cos\theta = \frac{\gamma_{\alpha\alpha}}{2\gamma_{\alpha\beta}}$$

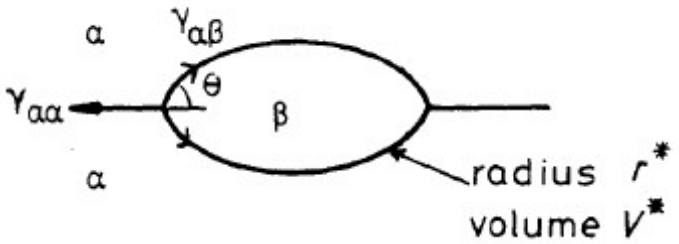


The excess free energy associate with the embryo is ,

$$\Delta G = -V\Delta G_V + A_{\alpha\beta}\gamma_{\alpha\beta} - A_{\alpha\alpha}\gamma_{\alpha\alpha}$$

$\Delta G_d$

Where V is volume of embryo, $A_{\alpha\beta}$ is are of α/β interface with the energy $\gamma_{\alpha\beta}$ created and $A_{\alpha\alpha}$ the are of α/α grain boundary of energy $\gamma_{\alpha\alpha}$ destroyed during the process.

The critical radius of the spherical caps is independent of the grain boundary and given by

$$\gamma^* = \frac{2\gamma_{\alpha\beta}}{\Delta G_V}$$

The activation energy barrier for heterogeneous nucleation is

$$\frac{\Delta G^*_{het}}{\Delta G^*_{\text{hom}}} = \frac{V^*_{het}}{V^*_{\text{hom}}} = S(\theta)$$

Where S(θ) is a shape factor given by

$$S(\theta) = \frac{1}{2}(2+\cos\theta)(1-\cos\theta)^2$$

The ability of a grain boundary to reduce $\Delta G^*_{het}$ i.e. act a nucleation site, depends on cosθ , i.e. on the ratio of $\gamma_{\alpha\alpha}/2\gamma_{\alpha\,\beta}$.

V* and ΔG* can be reduced further by nucleation on a grain edge or corner.

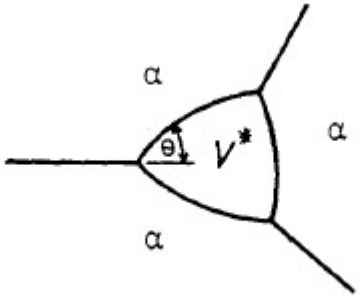


Critical nucleus shape for nucleation on a grain edge.


Critical nucleus shape for nucleation on a grain corner.

$\frac{\Delta G^*_{het}}{\Delta G^*_{\text{hom}}}$ depends on cosθ for various grain boundary nucleation sites.

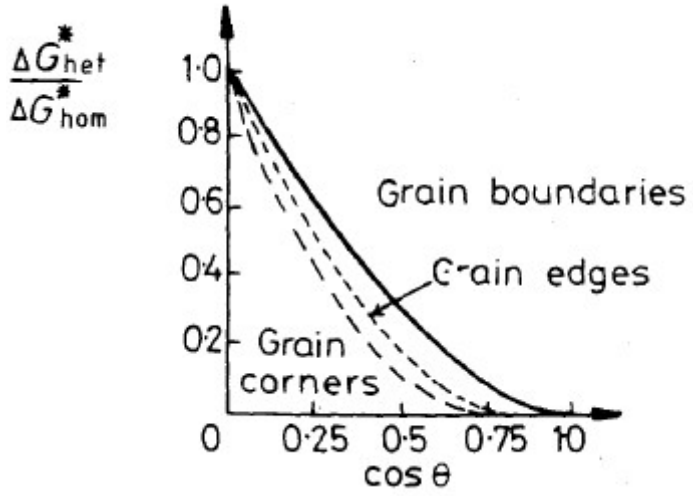

High-angle grain boundaries are effective nucleation site for incoherent precipitates with high $\gamma_{\alpha\beta}$.

If the matrix and precipitate are sufficiently to allow the formation of lower energy facets then V* and ΔG* can be further reduced.

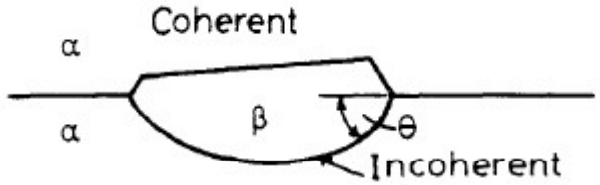


Fig. 5.10 The critical nucleus size can be reduced even further by forming a low-energy coherent interface with one grain.

Coherent nucleus have orientation relationship with one of the grains. Such nuceli form most rapidly due to smallest nucleation barrier.

Other planar defects such as inclusion/matrix interfaces, stacking faults and free surfaces behave similar way to grain boundaries. Stacking faults are less potent site compared to high-angle boundaries.

**Rate of heterogeneous Nucleation:**

The sequence of nucleation sites which increases $\Delta G_d$ i.e. decreasing $\Delta G^*$ are,

1. Homogenous sites
2. Vacancies
3. Dislocations
4. Stacking faults
5. Grain boundaries and interphase boundaries (high angle bourndaries)
6. Free surfaces.

The concentration of heterogenous nucleation sites is $C_1$ per unit volume, then the heterogeneous nucleation rate is

$$N_{\text{hom}} = \omega C_1 \exp\left(-\frac{\Delta G_m}{kT}\right)\exp\left(-\frac{\Delta G^*}{kT}\right) \quad \text{nucleim}^{-3}\text{s}^{-1}$$

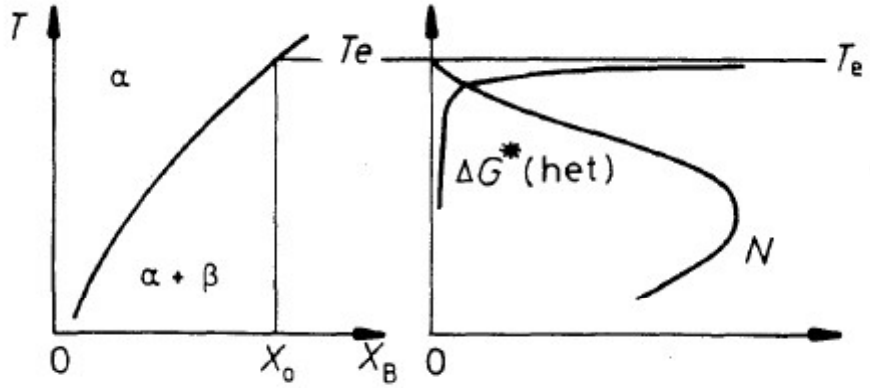


Fig. 5.12 The rate of heterogeneous nucleation during precipitation of β in alloy $X_0$ as a function of undercooling.

# Overall Transformation Kinetics – TTT Diagrams

TTT diagram

## Figure: TTT Diagram for plain carbon eutectoid steel

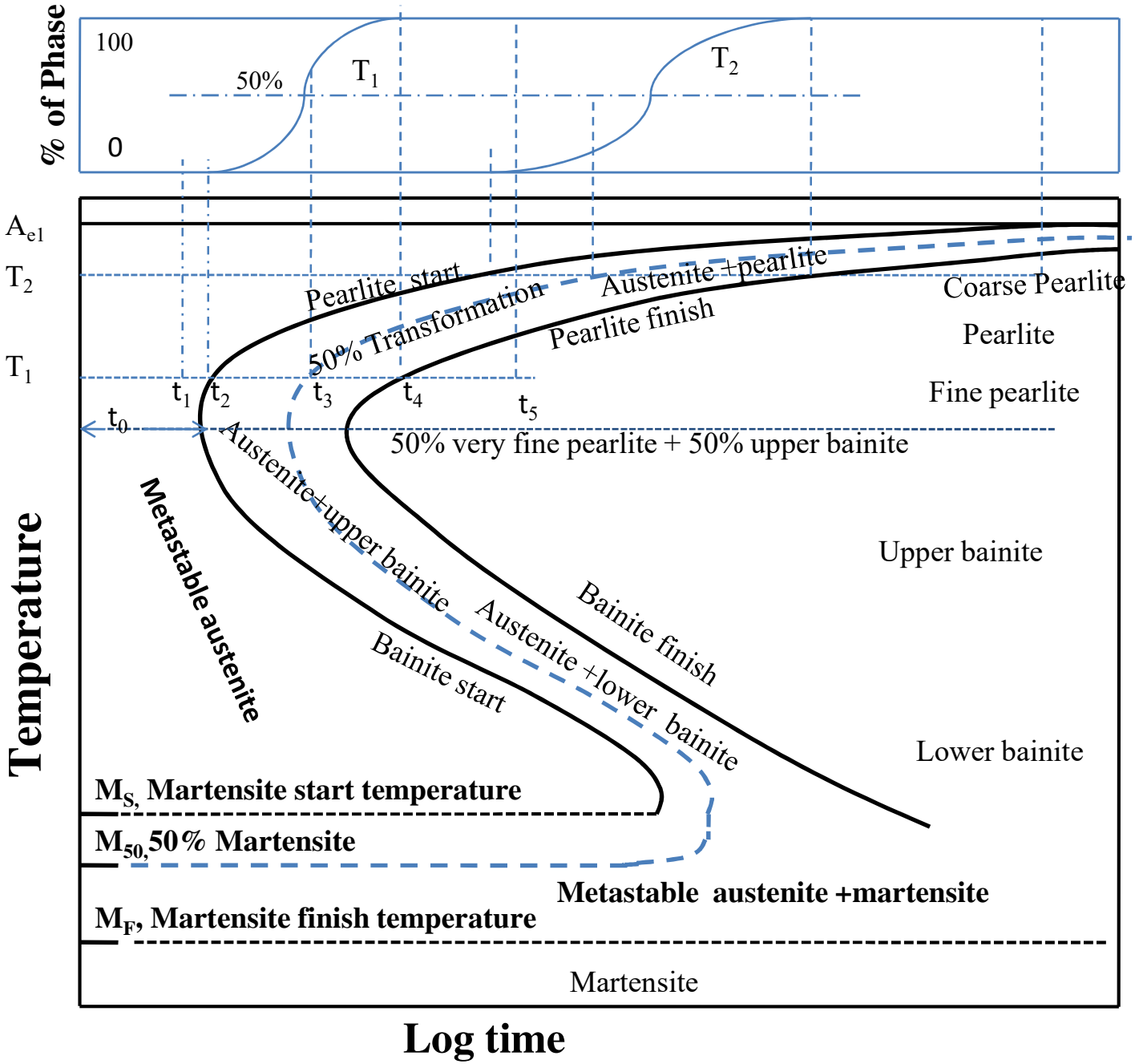


At $t_1$, incubation period for pearlite, $t_2$, pearlite starting time

Pearlite finish time $=t_4$

Minimum incubation period $t_0$ at the nose of the TTT diagram,

$M_S$=Martensite start temperature

$M_{50}$=temperature for 50% martensite formation

$M_F$= martensite finish temperature

# Overall Transformation Kinetics – TTT Diagrams

- The factors that determine f(t, T) are
  - Nucleation rate
  - Growth rate
  - Density and distribution of nucleation site
  - Overlap of diffusion field from adjacent transformed volumes
  - Impingement of adjacent transformed volumes.

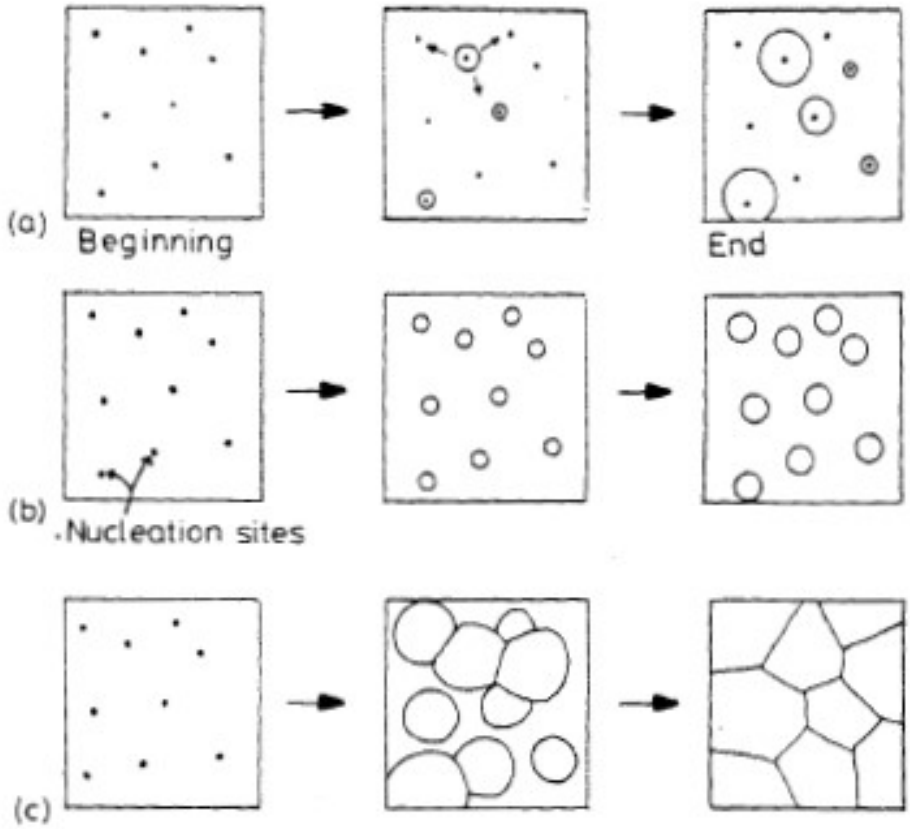


Fig. 5.24 (a) Nucleation at a constant rate during the whole transformation. (b) Site saturation—all nucleation occurs at the beginning of transformation. (c) A cellular transformation.

a) Nuclei form throughout the transformation. f will depend on nucleation rate and growth rate.

b) All the potential sites are consumed in the beginning known as site saturation. f will depend on the no. of nucleation site and growth rate.

c) All the parent phase is consumed is called as cellular transformation. Ex. : $\alpha \rightarrow \beta$ or $\alpha \rightarrow \beta + \gamma$. Pearlite, celluar precipitation, massive transformations and recrystallization are belong to this category. In this case, transformation terminate by impingement of adjacent cell which is growing with constant velocity.

For cellular transformation, the rate of supercritical nucleus (f) is,

$$f = 1 - \exp\left(-\frac{\pi}{3} N v^3 t^4\right)$$

Johnson-Mehl-Avrami Equaiton

N is nucleation rate, v is growth rate and t is time. The above equation is written as,

$$f = 1 - \exp\left(-kt^n\right)$$

n is numerical constant (value vary from ~1 to 4) and independent of temperature. k =$\pi Nv^3/3$. *K* depends on nucleation and growth rate and sensitive to temperature.

- Temperature close to T2, the friving force for transformation is very small. Hence both nucleation and growth rates are slow. Long time is required completion of transformation.
- When ΔT is very large, slow diffusion rate limit the rate of transformation.
- A maximum rate nucleation and growth takes place at intermediate temperatures.

# Precipitation in Age Hardening Alloys

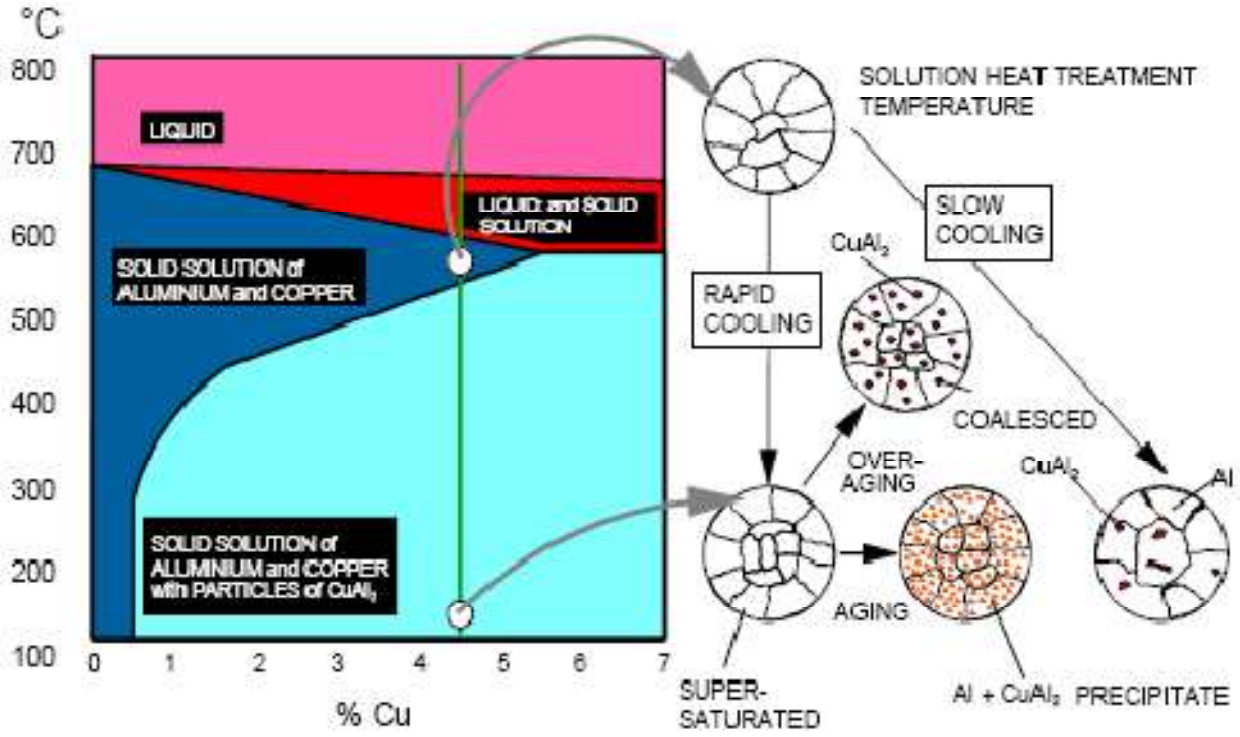

# Al-Cu precipitation sequence

- In precipitation-strengthened Al-Cu alloys, four intermediated structure are identified:
    1. $Gp_1$ (Guiner – Preston) zones
    2. $GP_2$ zone (θ’’)
    3. θ’ and
    4. θ ($CuAl_2$)

# Al-Cu ppt. structures

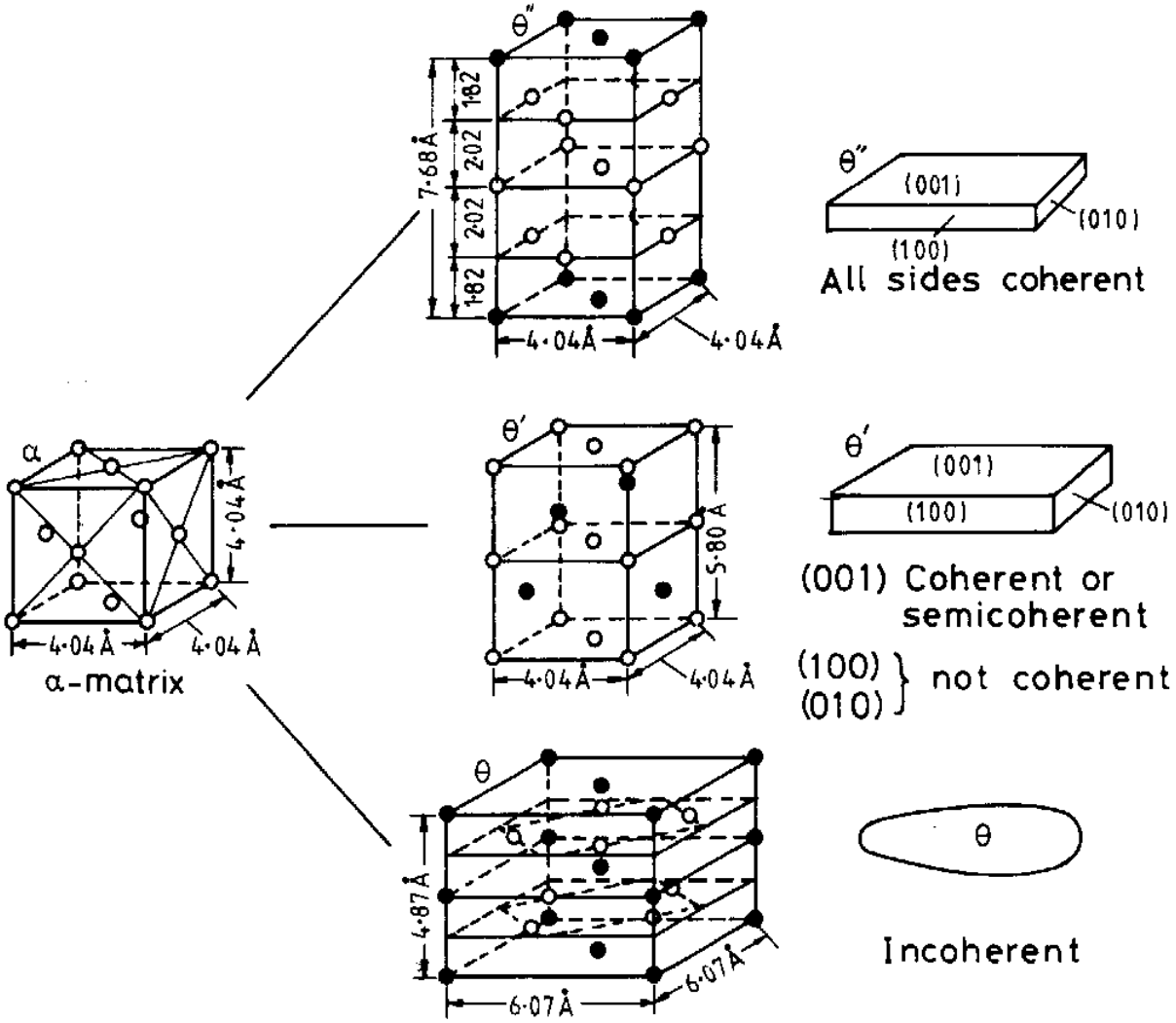


Fig. 5.29 Structure and morphology of θ″, θ′ and θ in Al–Cu (○ Al, ● Cu).

- GP zone is fully coherent with the matrix. Hence very low interfacial energy.
- θ phase is complex tetragonal crystal structure which have high energy incoherent interfaces.

# Al-Cu precipitation sequence

- The sequence is:

$$\alpha_0 \rightarrow \alpha_1 + \text{GP-zones} \rightarrow \alpha_2 + \theta'' \rightarrow \alpha_3 + \theta' \rightarrow \alpha_4 + \theta$$

The phase are:

$\alpha_n$ – fcc solid solution of Al; $n^{th}$ subscript denotes each equilibrium

GP zones - mono-atomic layers of Cu on $(001)_{Al}$

θ“ - thin discs, fully coherent precipitate with matrix

θ’ - disc-shaped, semi-coherent precipitate.

θ - incoherent interface, ~spherical, complex BCT structure precipitate.

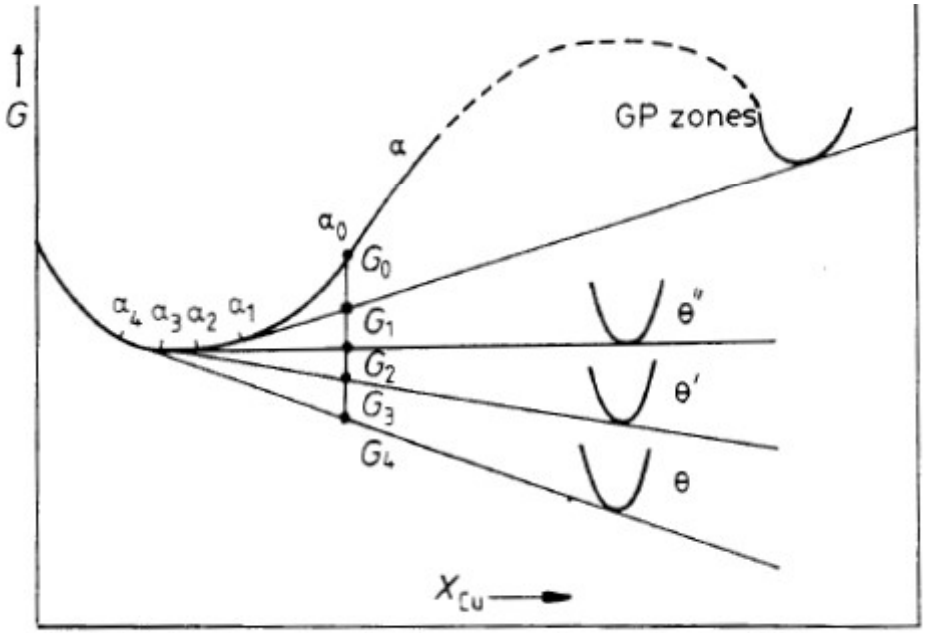


Fig. 5.27 A schematic molar free energy diagram for the Al–Cu system.

The free energy of the alloy sequence decreases as,

$G_o \rightarrow G_1 \rightarrow G_2 \rightarrow G_3 \rightarrow G_4$.

Transformation stops when the minimum free energy equilibrium state $G_4$ is reached. i.e. $\alpha_4+\theta$.

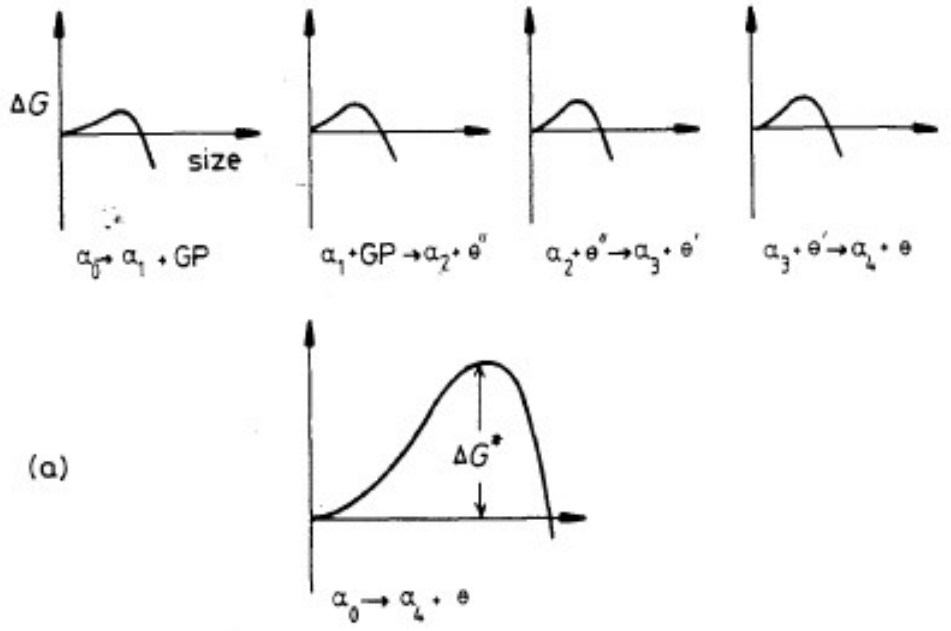


Transition phases forms before equilibrium phases due to lower activation energy barrier for nucleation.

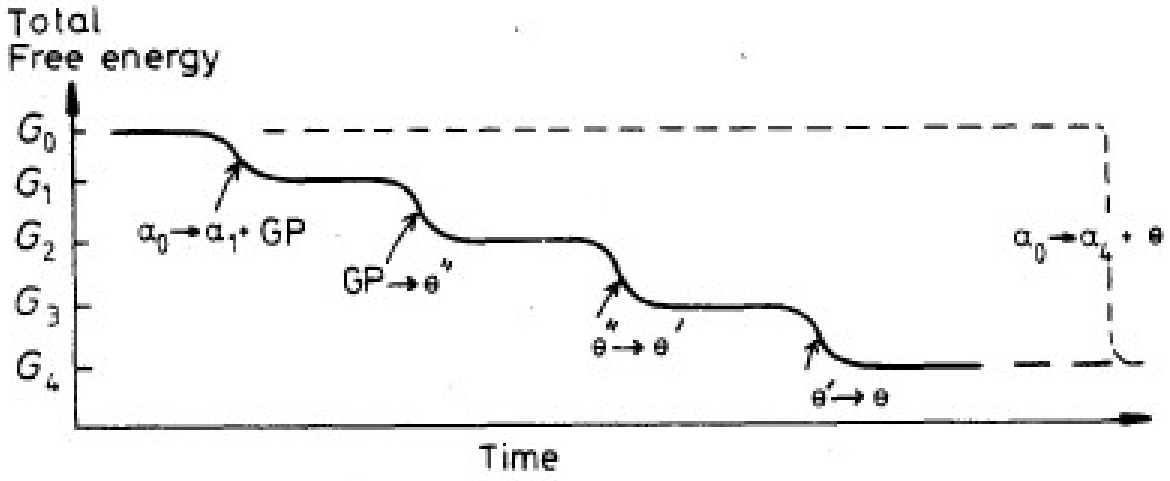


Schematic diagram showing the total free energy of the alloy with respect time

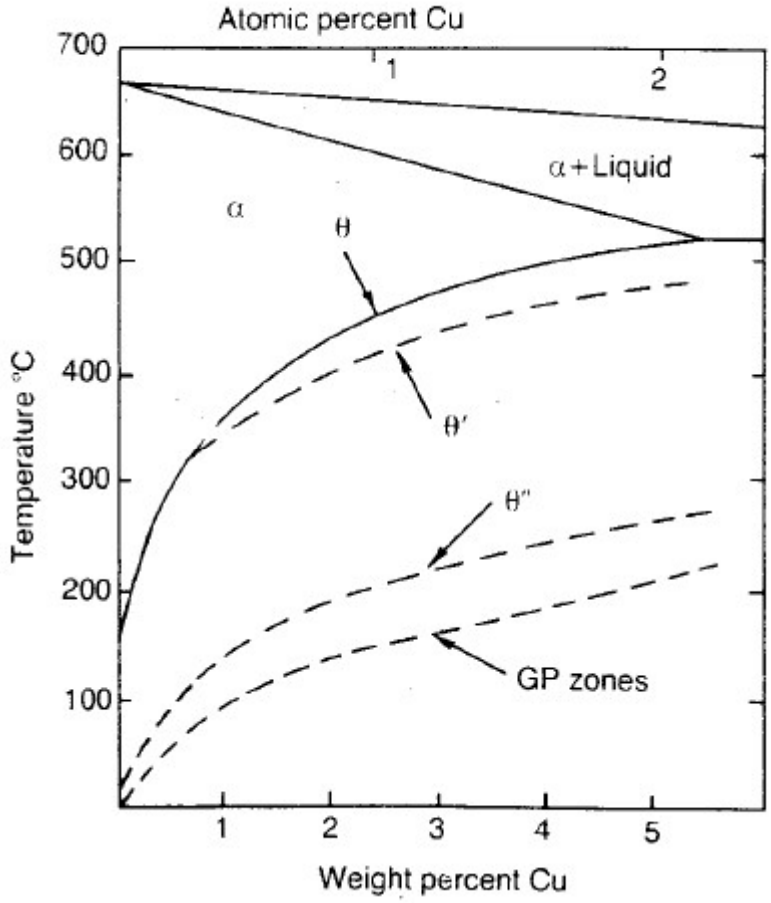


Al-Cu phase diagram showing the metastable phases solvuses.

# Al-Cu phase relationships

The explanation of age hardening depends on understanding the metastable phases that can appear.

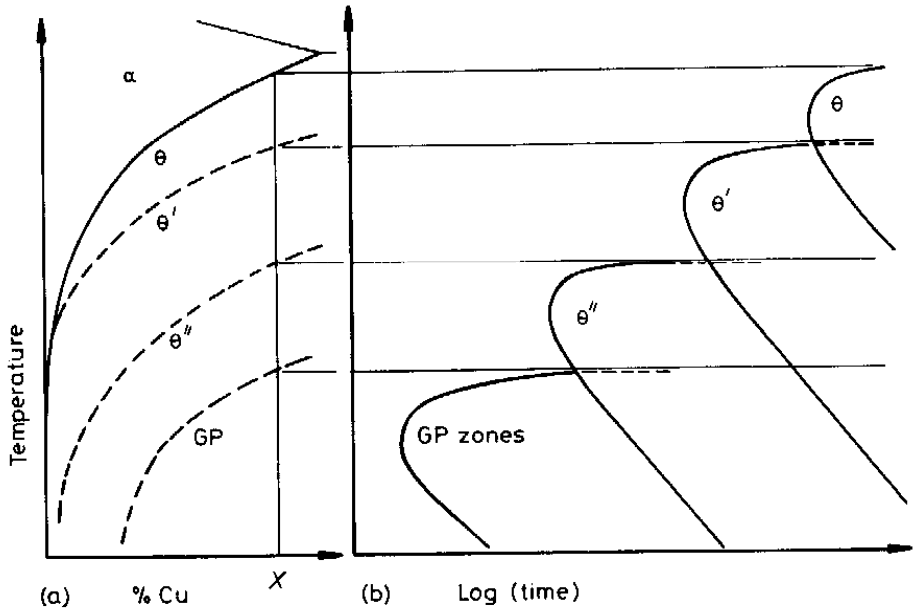


Fig. 5.32 (a) Metastable solvus lines in Al–Cu (schematic). (b) Time for start of precipitation at different temperatures for alloy $X$ in (a).

# Age Hardening

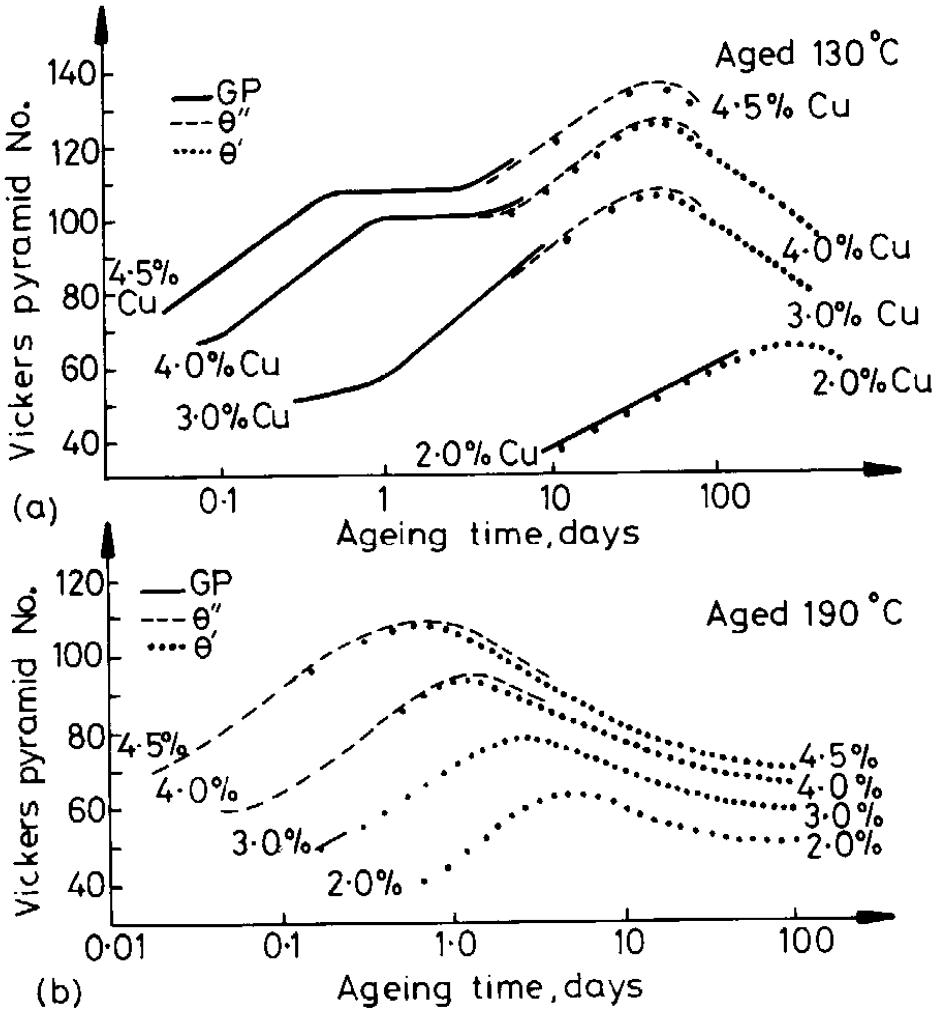


Fig. 5.37 Hardness v. time for various Al–Cu alloys at (a) 130 °C (b) 190 °C. (After J.M. Silcock. T.J. Heal and H.K. Hardy, *Journal of the Institute of Metals* **82** (1953–1954) 239.

Overaging: . After the peak hardness, further ageing tends to decrease the hardness.

# Pearlitic Transformation

- At eutectoid composition (0.77% C)

  $Fe_3C$ – 11.28 %  α-Ferrite- 88.72%

  Density =7.70 g/cc  density = 7.87 g/cc

- Decomposition of austenite to pealite is
  - Diffusion controlled process
  - Nucleation and growth
  - Interlamellar spacing depends on transformation temp.

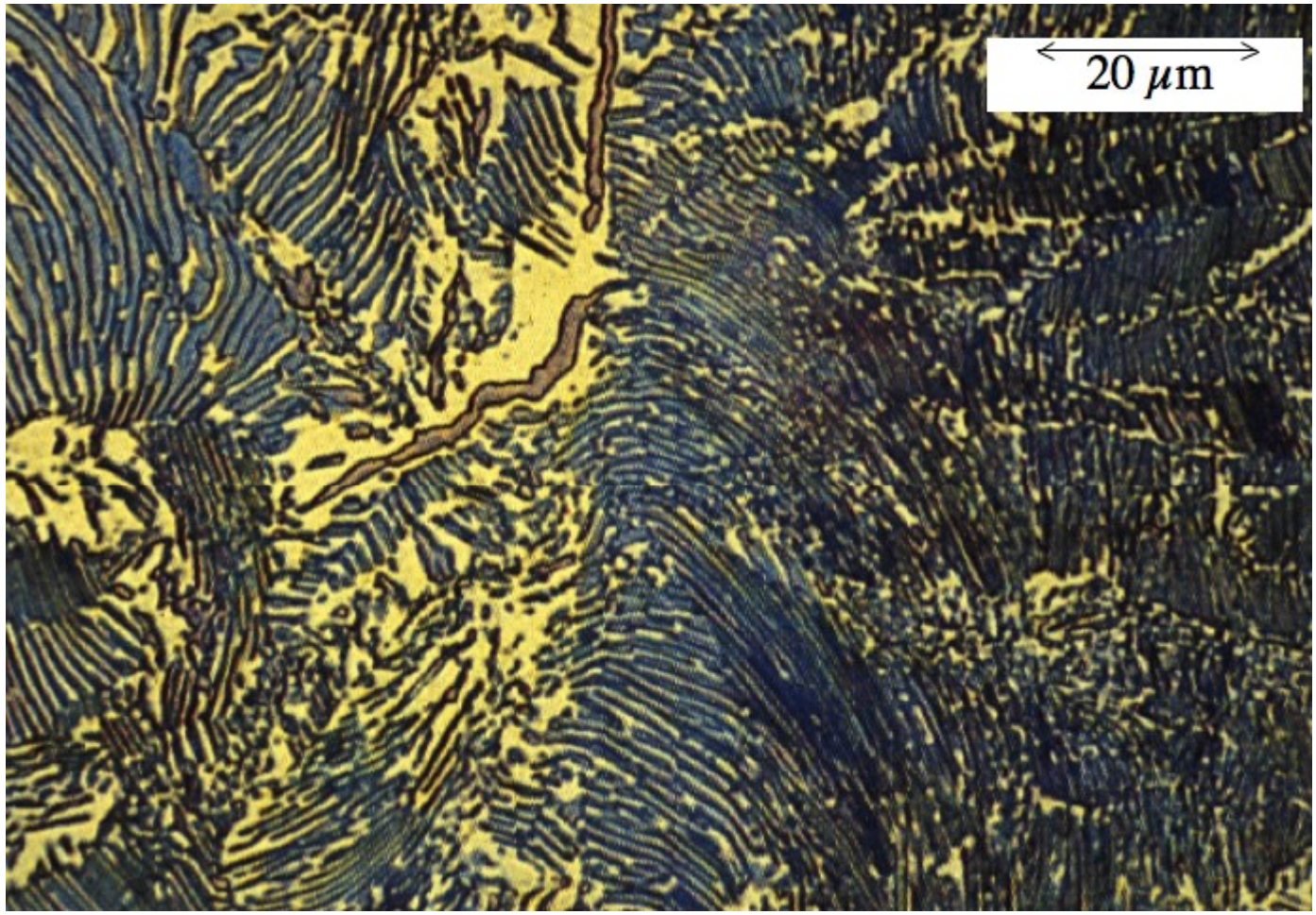


Figure : The appearance of a (coarse and fine) pearlitic microstructure under optical microscope.

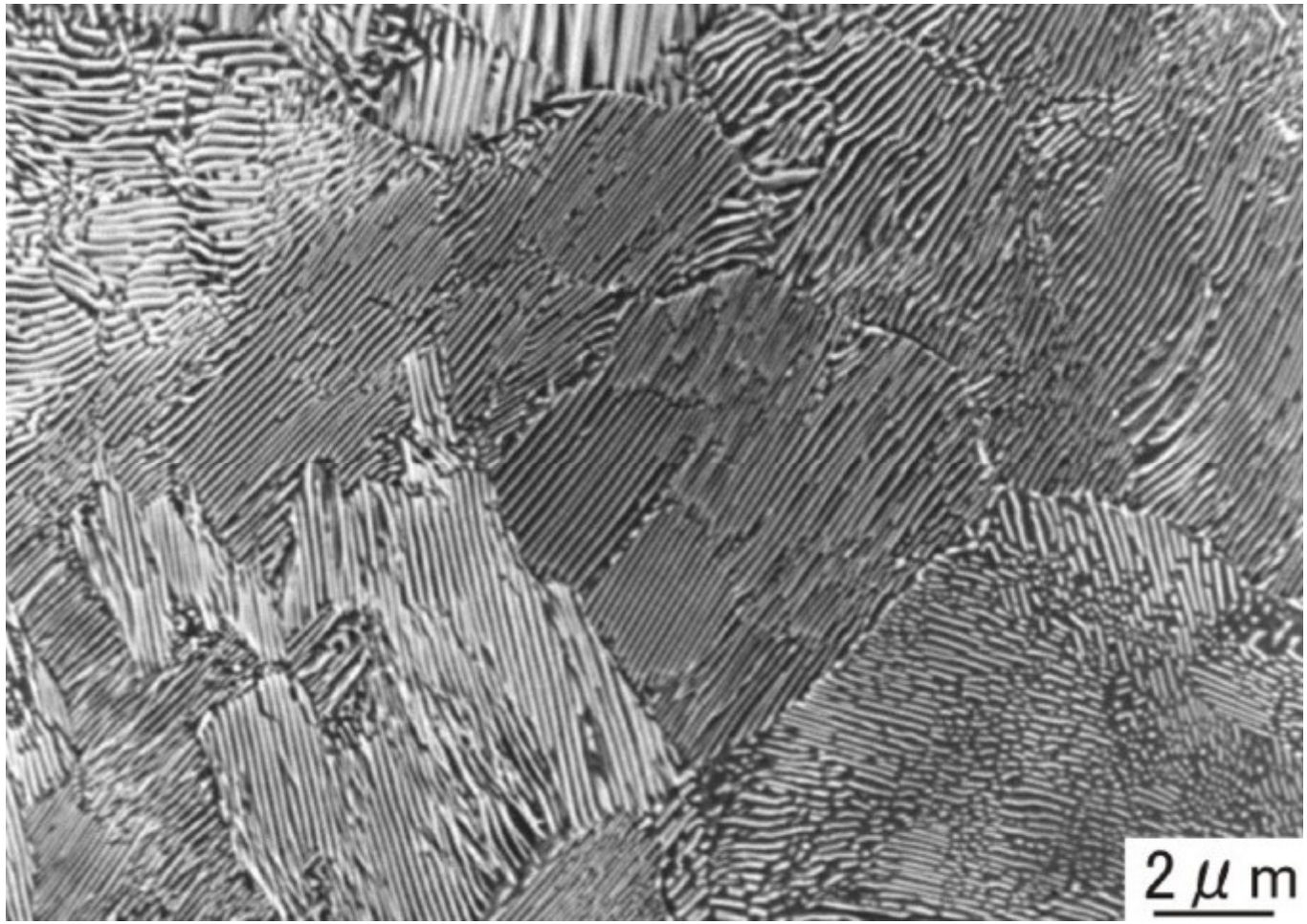


Figure: Optical micrograph showing colonies of pearlite

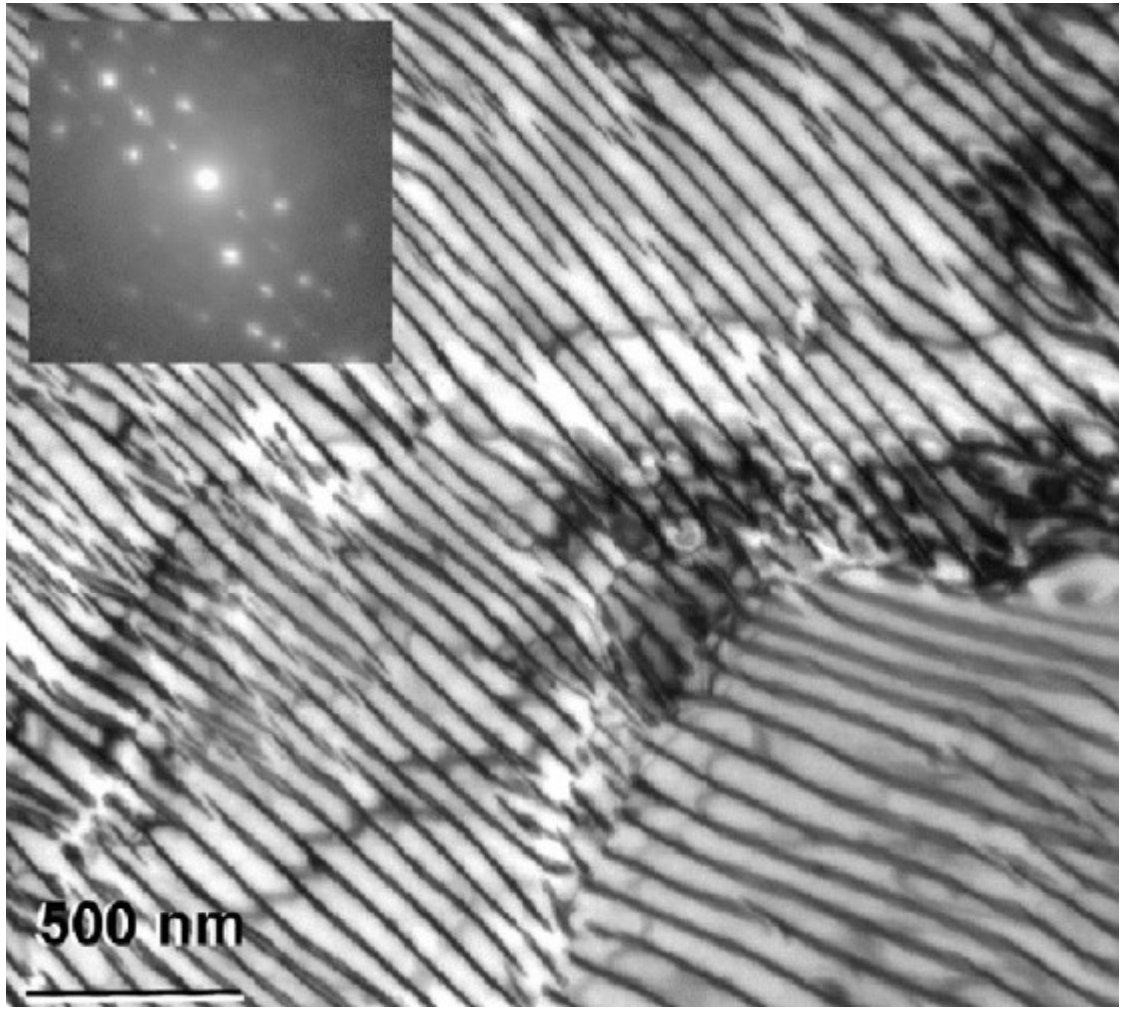


Figure: Transmission electron micrograph of extremely fine pearlite.

# Hull-Mehl model

Nucleation and growth of pearlite

(a) Initial $Fe_3C$ nucleus;

(b) $Fe_3C$ plate full grown, α-Fe now nucleated;

(c) α-Fe plates now full grown, new $Fe_3C$ plates nucleated;

(d) $Fe_3C$ nucleus of different orientation forms and original colony grows;

(e) New colony at advanced stage of growth

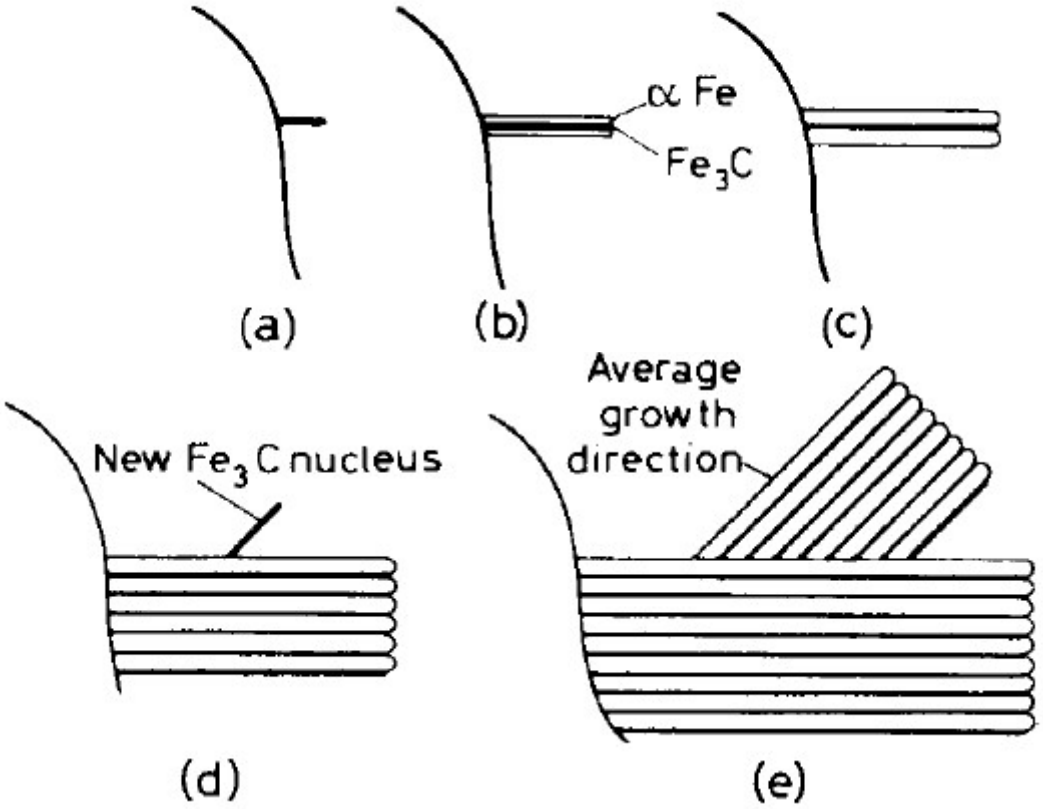

Fig. 5.56 A partially transformed eutectoid steel. Pearlite has nucleated on grain boundaries and inclusions (× 100). (After J.W. Cahn and W.C. Hagel in *Decomposition of Austenite by Diffusional Processes*, V.F. Zackay and H.I. Aaronson (Eds.), 1962, by permission of The Metallurgical Society of AIME.)

A partially transformed eutectoid steel

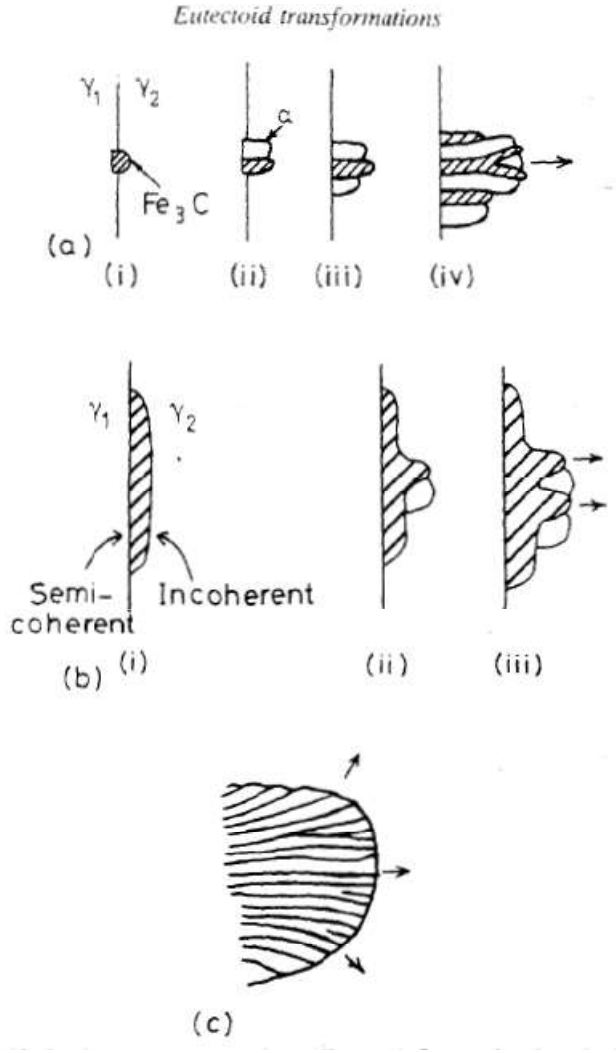


a) Transformation of eutectoid steel
b) Transformation of hypereutectoid steel

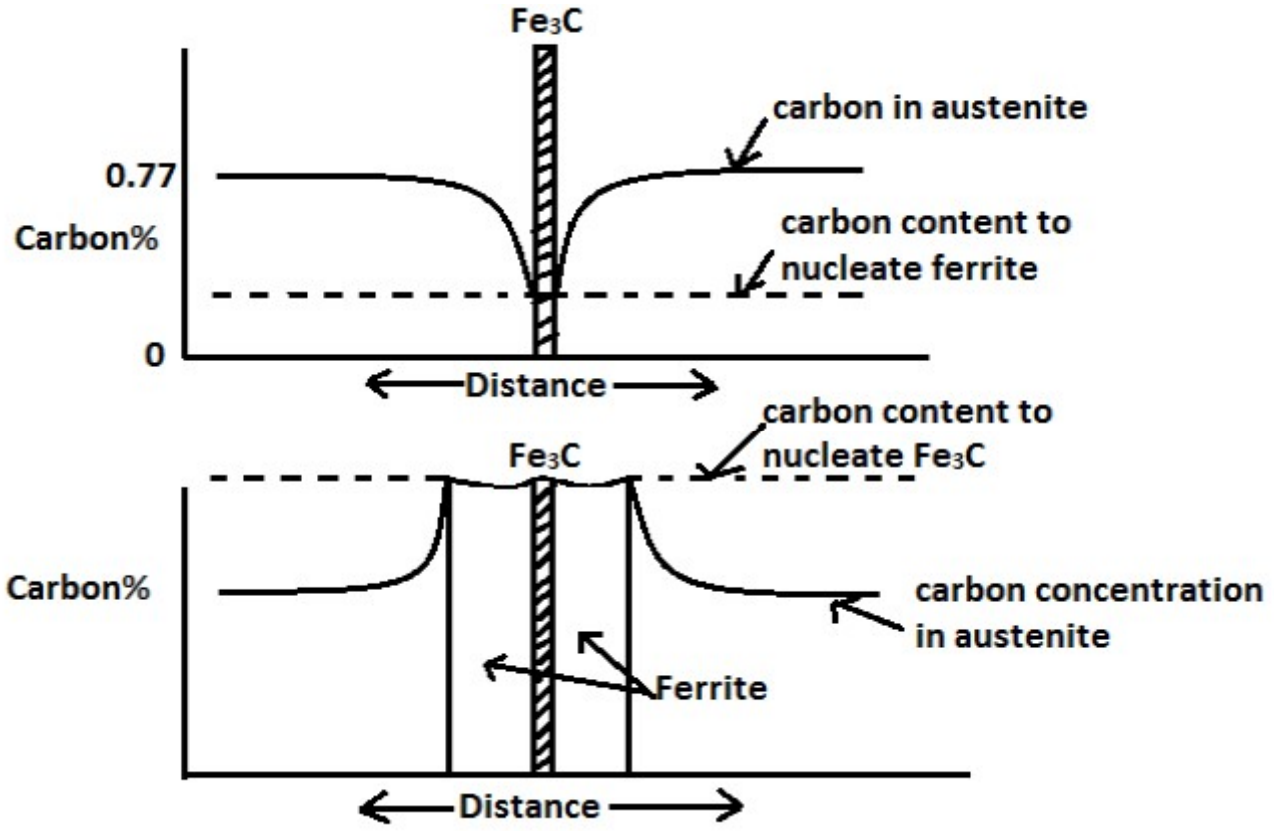
Fe3C
carbon in austenite
0.77
Carbon%
carbon content to
nucleate ferrite
0
Distance
carbon content to
nucleate Fe3C
Fe3C
Carbon%
carbon concentration
in austenite
Ferrite
Distance

# Transformation of Austenite to Pearlite

- The decomposition of austenite into pearlite by diffusion controlled process. i.e. Diffusion of C. It can be explained by Thermodynamics and Kinetics
- There are two steps involved in diffusion controlled process
  - Nucleation
  - Growth
- The rate of transformation is governed by both.
- Rate of nucleation and growth is zero at $A_1$ temperature
- Rate of diffusion of C atoms is negligible below 200˚C.

## Thermodynamics and Kinetics of transformation:

At $Ac_1$, G(pearlite) = G(austenite) → No transformation

$<Ac_1$, G(pearlite) < G(austenite)

austenite ⟹ pearlite

$<< Ac_1$, stability of pearlite increases

Rate of austenite to pearlite transformation increases with lowering / undercooling transformation temperature

Rate of diffusion of carbon decreases exponent with decreasing temperature

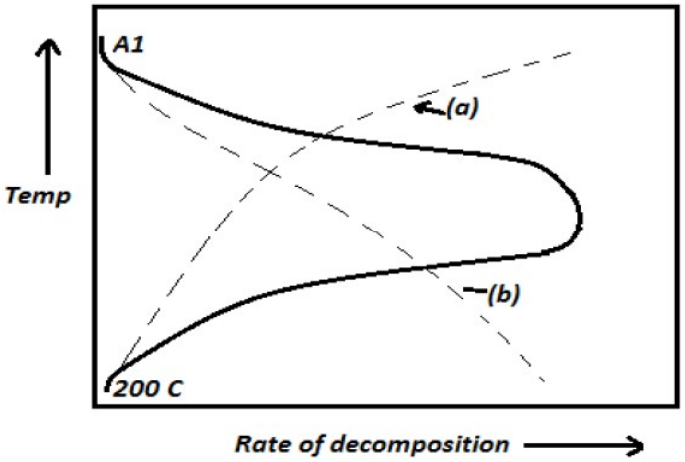


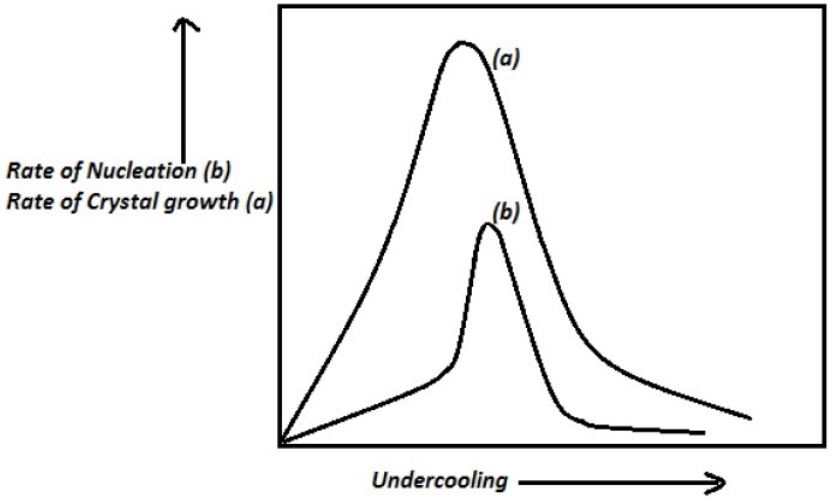


a) Rate of crystal growth
b) Rate of nucleation

The rate of nucleation and growth with respect to under cooling

# Interlamellar spacing:

- Zener has shown that

$$S_o = \frac{4\gamma T_m}{\Delta H \Delta T}$$

Where γ – specific surface energy,
$T_m$- transformation temperature,
ΔH – enthalpy of transformation
ΔT- amount of under cooling .

- Depends on function of transformation temperature.
- Lower the transformation temp., smaller is the interlamellar spacing.
- Hardness and strength increases when $S_o$ decrease.

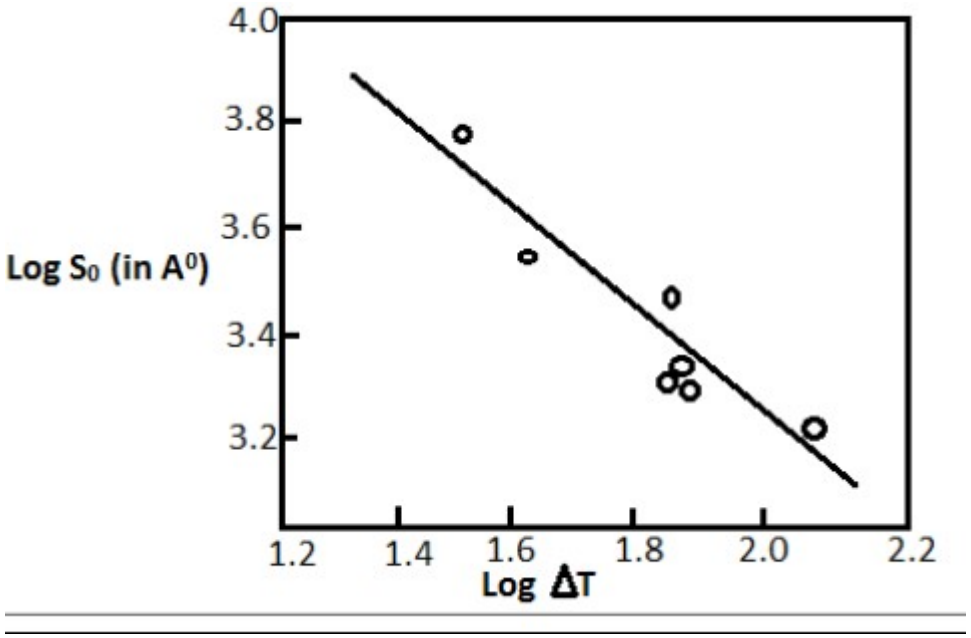

# Cellular Precipitation

- Cellular /discontinuous precipitation: The composition of the matrix changes discontinuously as the cell front passes.

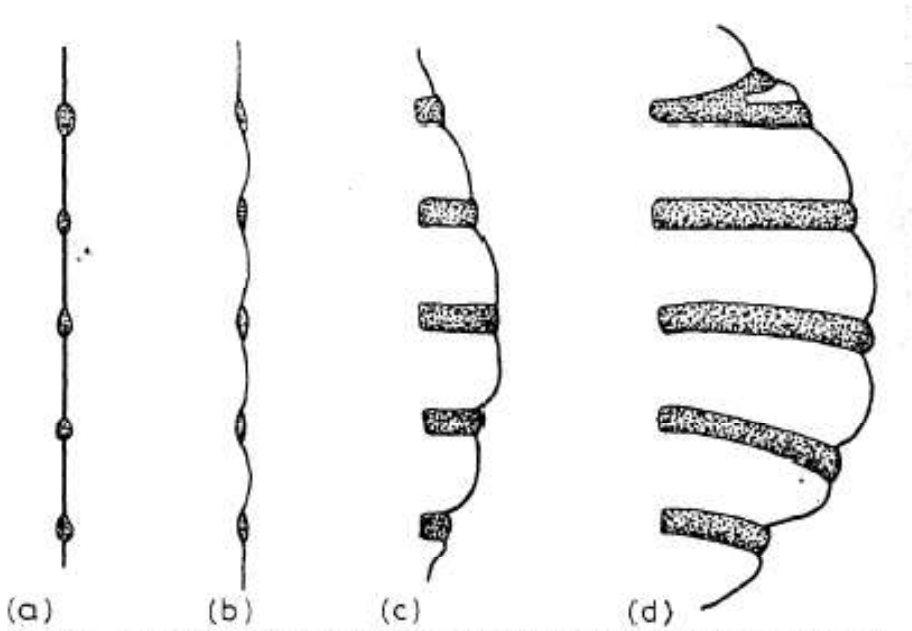


Fig. 5.50 A schematic diagram showing a possible sequence of steps during the development of cellular precipitation.

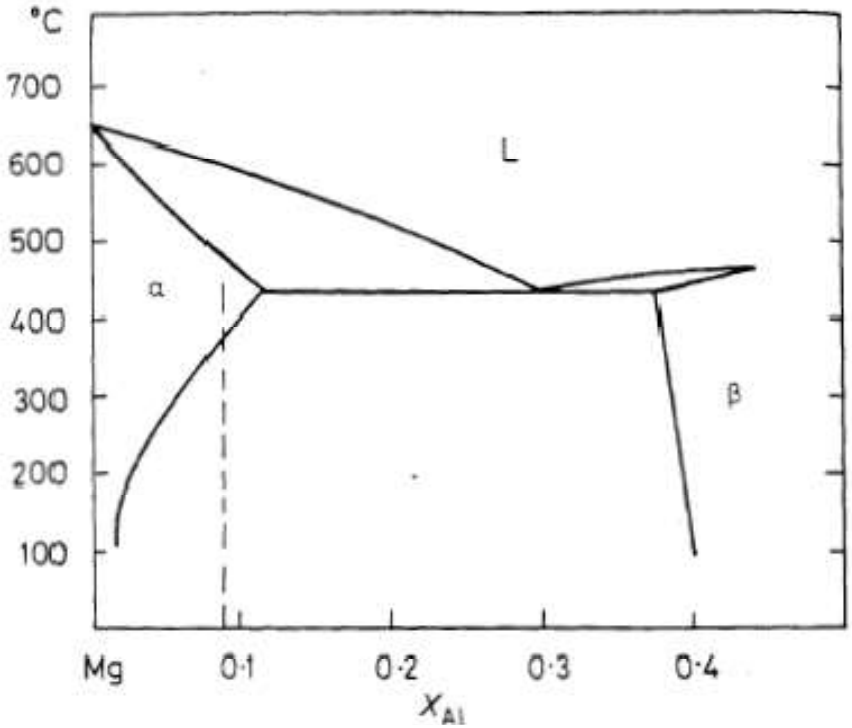


Mg-Al Partial Phase Diagram

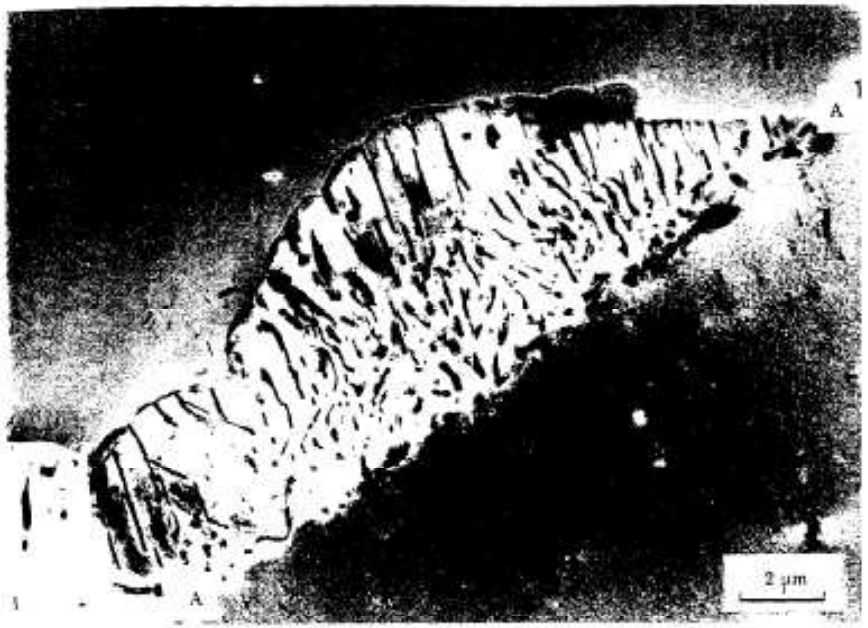


Fig. 5.51 Cellular precipitation of $Mg_{17}Al_{12}$ in an Mg–9 at% Al alloy solution treated and aged 1 h at 220 °C followed by 2 min at 310 °C. Some general $Mg_{17}Al_{12}$ precipitation has also occurred on dislocations within the grains.

The reaction is $\alpha' \rightarrow \alpha + \beta$

Where α' -- supersaturated matrix ,
α – same phase with less solute,

β -- Precipitate

In Mg- 9at.% Al,

$\alpha' \rightarrow \alpha + Mg_{17}Al_{12}$

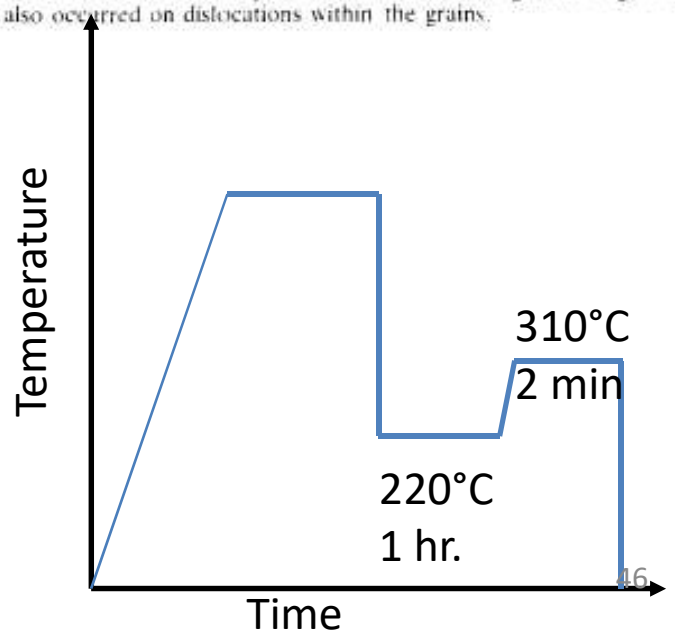


Fig. 5.53 A cell formed during ageing at two temperatures: 30 min at 220 °C followed by 30 min at 277 °C and water quenched. Note the change in interlamellar spacing caused by the change in undercooling.

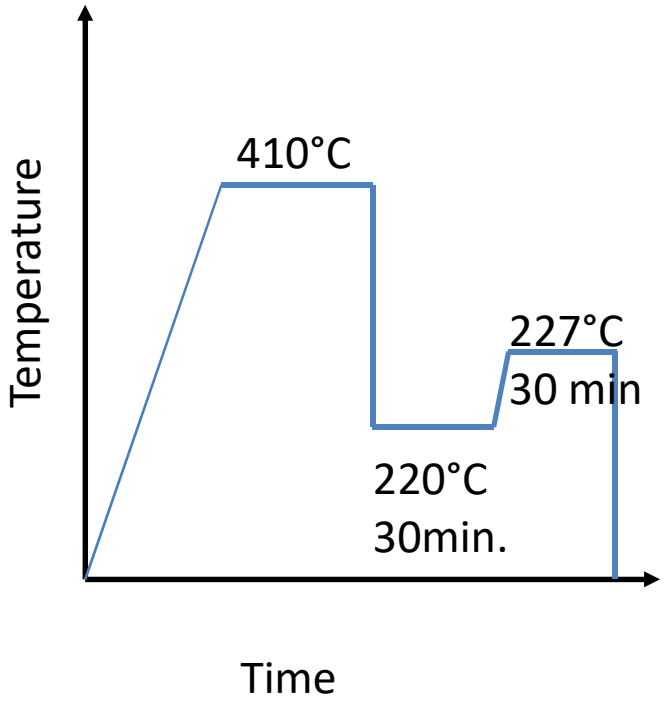


- Interlamellar spacing is higher at higher aging temperature. It is mainly due to less free energy is available for the formation of α/β interfaces when the total driving forces for transformation is reduced.

- The study of Mg-Al system using electron energy loss spectroscopy shows that solute diffusion via grain boundaries than though the lattice
- Cellular precipitation is also called as discontinuous precipitation because the composition of the matrix changes discontinuously as the cell front passes.

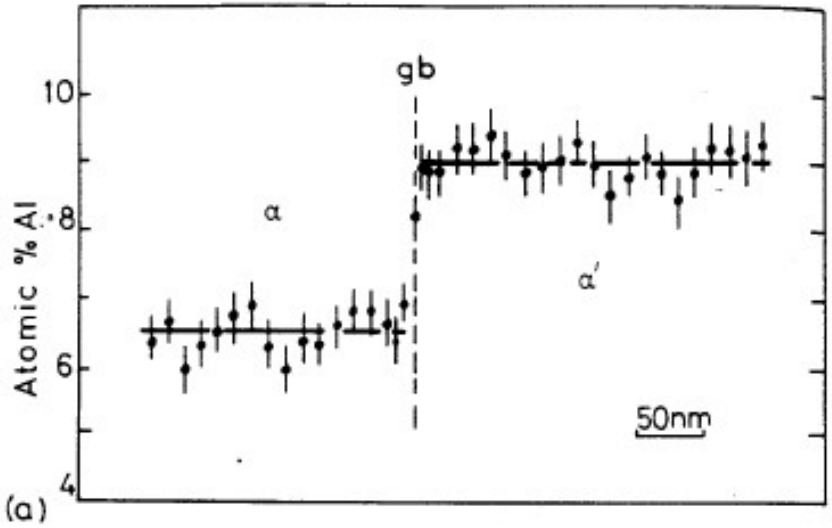


a) Variation of Al concentration across an advancing grain boundary midway between two precipitate lammelle

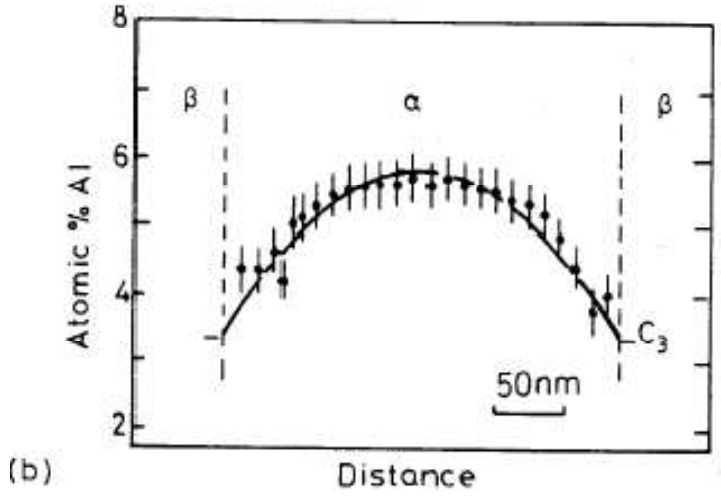


b) A similar profile along two precipitate

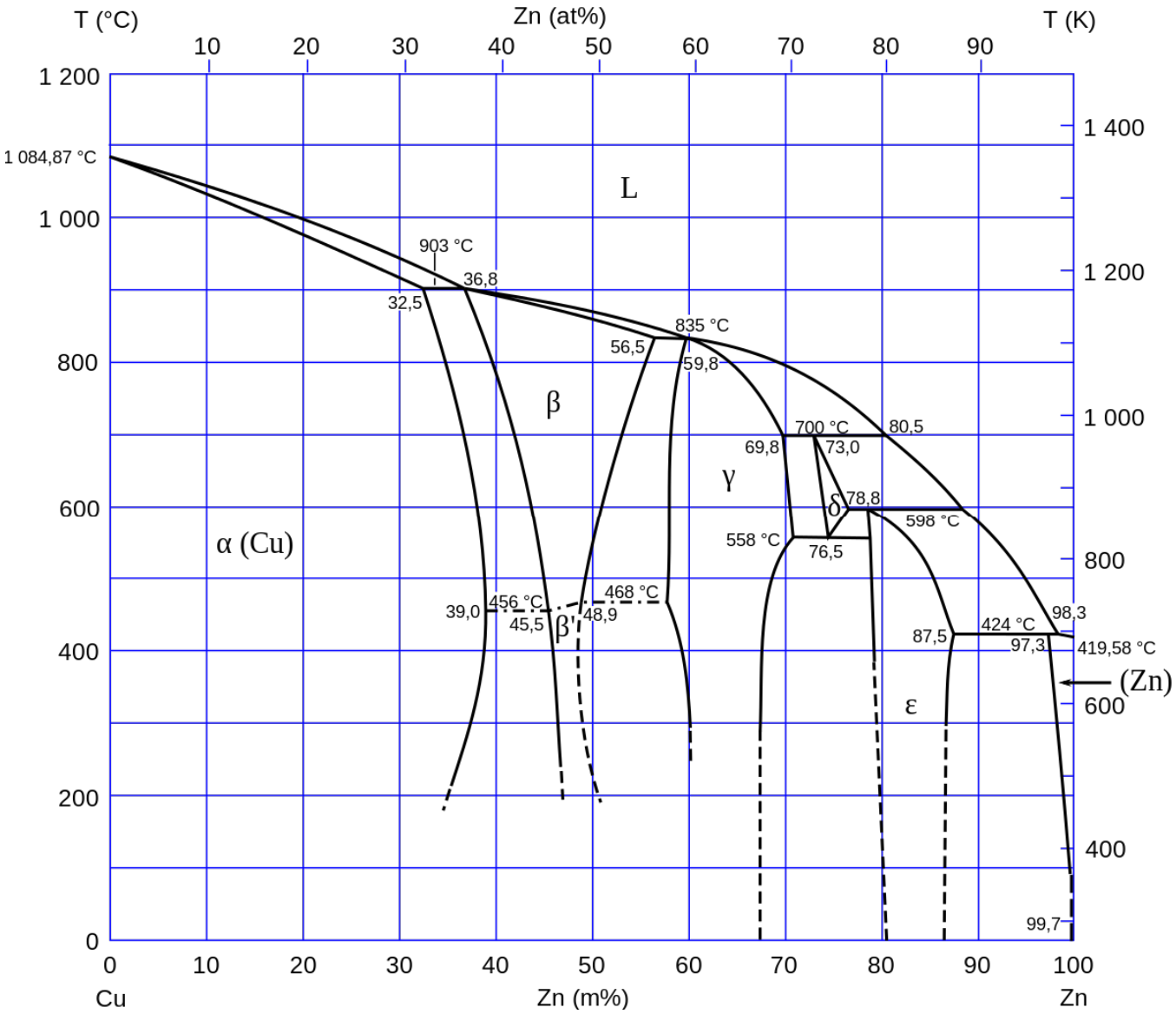
T (°C)
Zn (at%)
T (K)
10
20
30
40
50
60
70
80
90
1 200
1 000
800
600
400
200
0
1 400
1 200
1 000
800
600
400
1 084,87 °C
L
903 °C
36,8
32,5
835 °C
56,5
59,8
β
700 °C
80,5
69,8
73,0
γ
δ
78,8
598 °C
558 °C
76,5
α (Cu)
468 °C
456 °C
39,0
45,5
β'
48,9
98,3
424 °C
87,5
97,3
419,58 °C
(Zn)
ε
99,7
0
10
20
30
40
50
60
70
80
90
100
Cu
Zn (m%)
Zn

# Massive Transformations

In Cu-Zn phase diagram, alloy of Cu-38 at.%Zn alloy

T>~800˚C →β phase is stable

T<500˚C→ α phase is stable.

500-800˚C → α+ β phase is stable

The above transformation possible on slow cooling rate. Formation of α from β require long range diffusion of Zn moving away from α/β interfaces

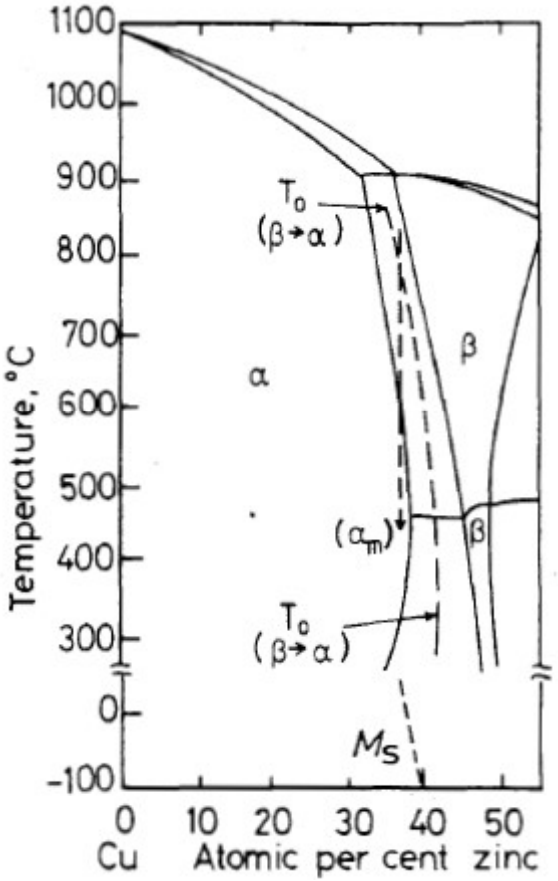

If the alloy is cooled fast using brine solution, β phase will be retained below 500˚C. Then β will transform into α in the same composition. It is called as massive transformation.

- Massive α grains nucleate at grain boundaries and grow rapidly into the surrounding β.
- Due to rapid growth α/β boundaries, has irregular appearance.
- massive α grows without the need for long-range diffusion.

- Massive transformation is also called as a diffusionless civilian transformation. Hence growth only involves thermally activated jumping across the α/β interface.

Massive α formed at the grain boundaries of β in Cu-38.7wt.%Zn quenched from 850˚C in brine at 0˚C

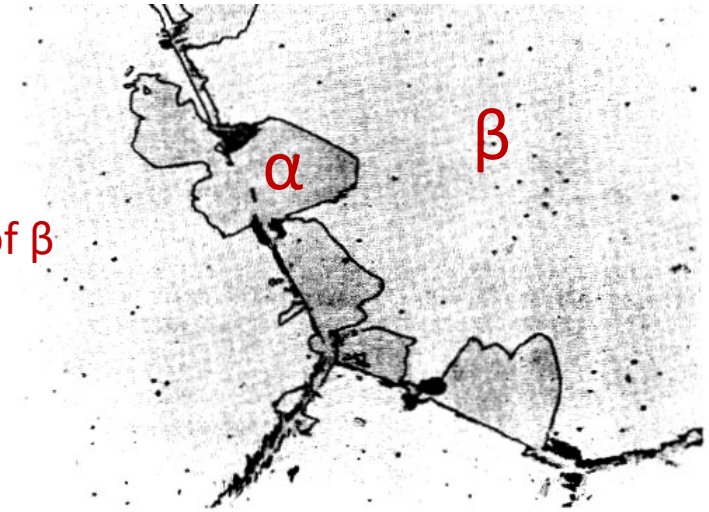

- Martensite transformation is diffusionless military transformation i.e . β is sheared into α by the cooperative movement of atoms across a glissile interface.
- In Massive transformation, growth of α involves thermally activated interface migration.
- For Martensite transformation, quench rate is high. In Cu-Zn alloy Ms temperature is below 0˚C.

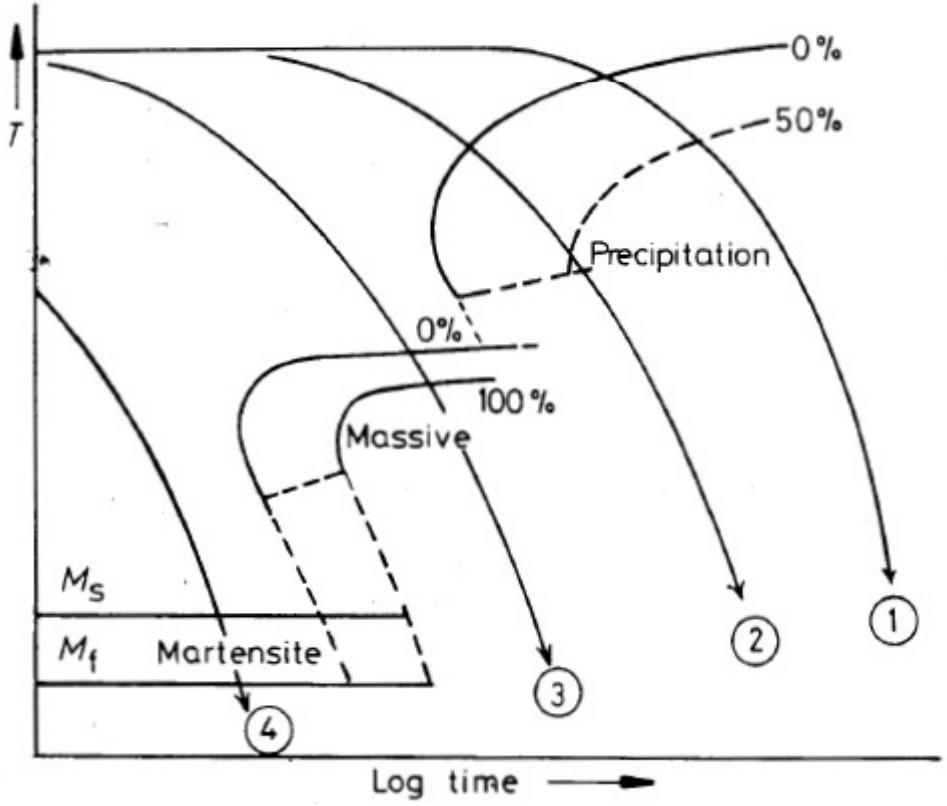


A possibel CCT diagram for systems showing a massive transformation. Slow cooling (1) produces equixed α. Widmanstatten morphologies result from faster cooling (2). Moderately rapid quenching (3) produces the massive transformation. While the highest quench rate (4) leads to martensite transformation

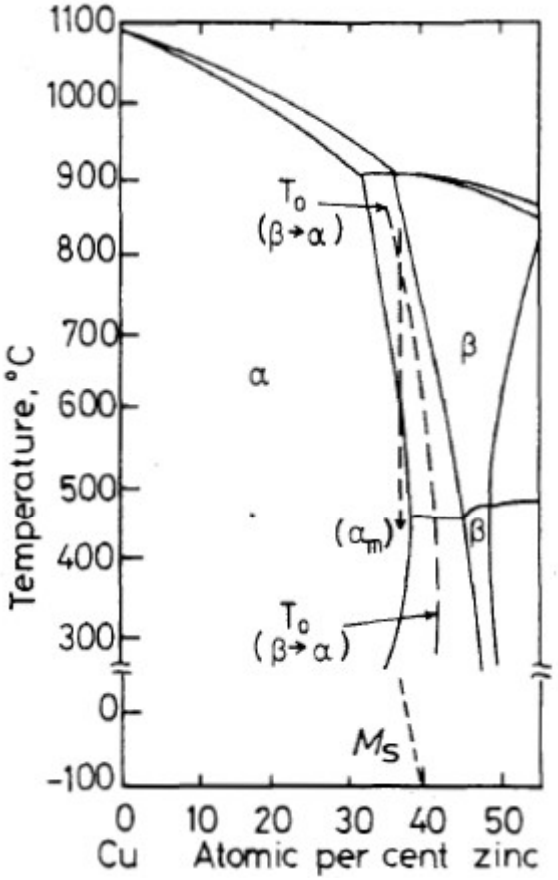


Cu-Zn Phase diagram

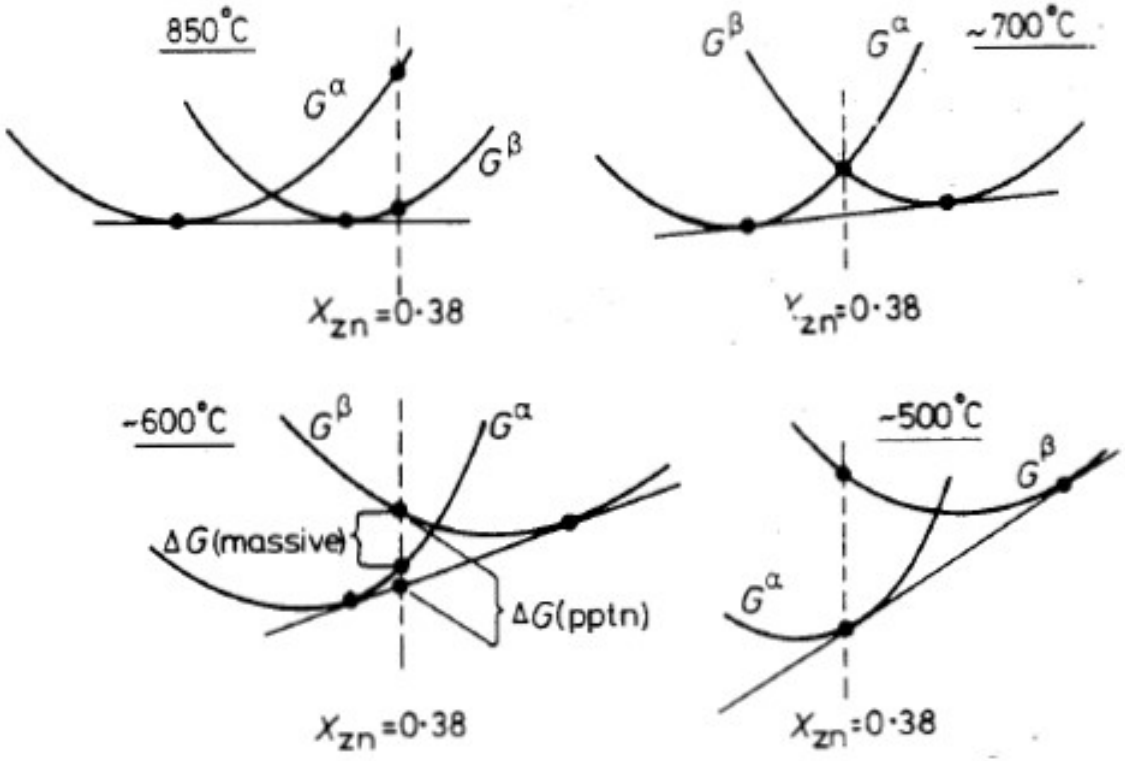


A schematic representation of the free-energy composition curves for α and β in Cu-Zn system at various temperatures.

- For Massive transformation, Free energy of the new phase must be lower than the parent phase and both phases having the same composition.
- Massive transformations is observed in Cu-Al

# Ordering Transformation

In regular solution model, Solid solution having negative ΔHmix (Ω<0) prefer unlike atoms next to each other and have tendency to form ordered phases at low temperatures.

Main five types of ordered solutions are

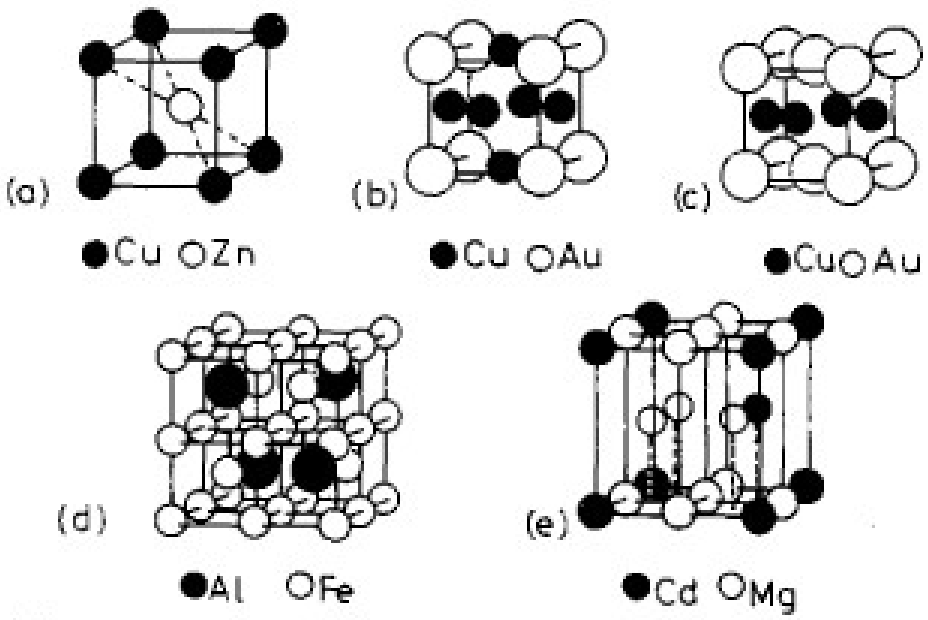


a) $L2_0$: CuZn, FeCo, NIAl, FeAl, AgMg
b) $L1_2$: Cu3Au, Au3Cu, Ni3Mn, Ni3Fe, Ni3Al, Pt3Fe
c) $L1_0$: CuAu, CoPt, FePt
d) $D0_3$:Fe3Al, Fe3Si, Fe3Be, Cu3Al
e) $D0_{19}$: Mg3Cd, Cd3Mg, Ti3Al, Ni3Sn

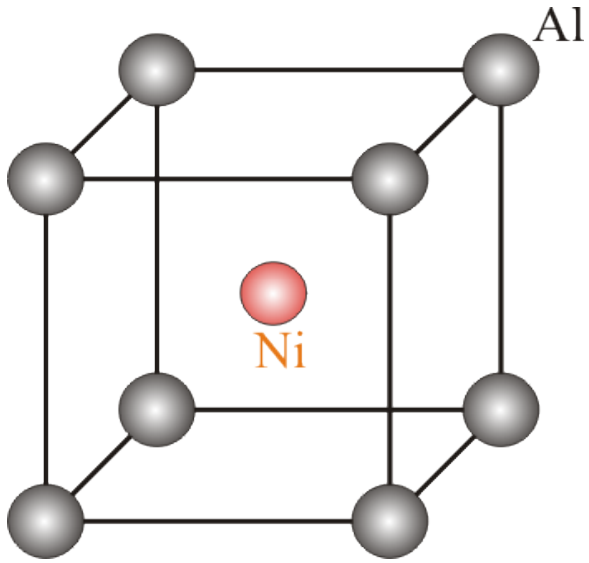
Al
Ni

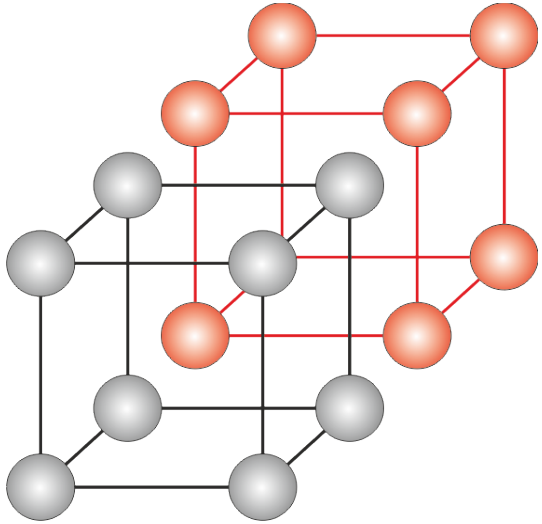

- Ordered β is stable at low temperature. At high temperature disordered β phase is stable
- Long range order parameter is

$$L = \frac{r_A - X_A}{1 - X_A} \; or \; \frac{r_B - X_B}{1 - X_B}$$

Where $X_A$ is mole fraction of A in the alloy and $r_A$ is the probability of atom A occupy by right kind of site.

L=1 → Highly ordered arrangement (lowest internal energy and $S_{conf.}$=0))

L=0 → disordered arrangement $S_{conf.}$=max.

As temp. Increases L decreases. The abrupt changes about observed in critical temperature ($T_c$)

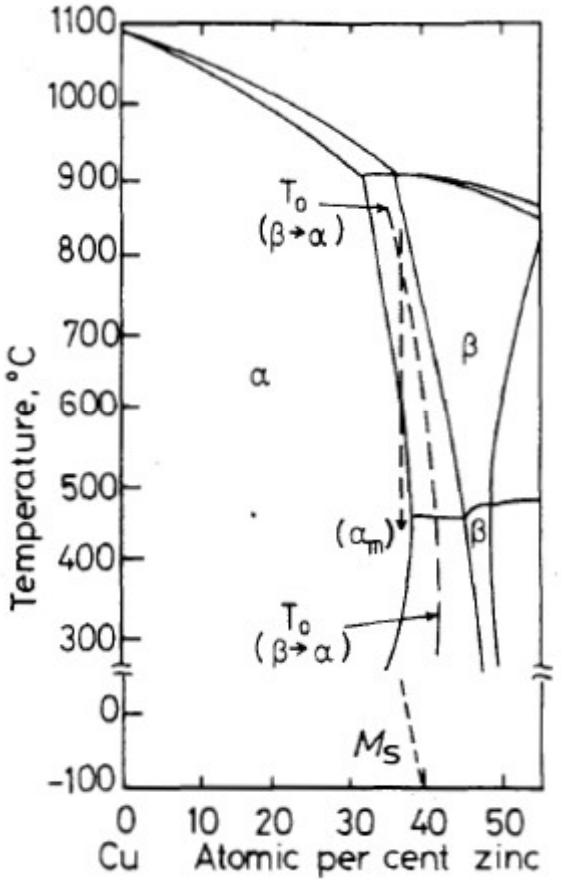

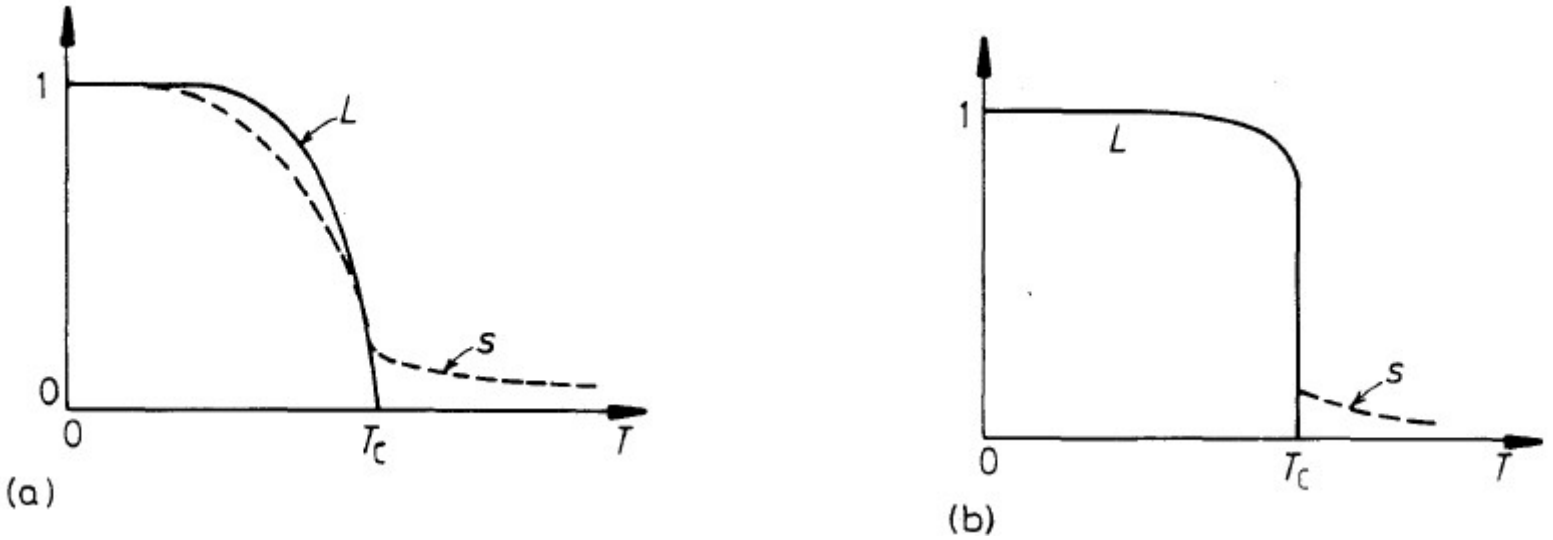


The variation of long-range order (L) and short-range order (s) for a) CuZn type and b) Cu3Au type transformation

T>Tc → L=0. but Ω<0, there is still tendency for atoms to attract unlike atoms for short distances. Hence it has short range order.

The difference in behavior is due to the different atomic configuration in the two superlattices.

## First Order Transformation

- Parent and product are different phases.
- Discontinuous changes in entropy, enthalpy and specific volume.
- Latent heat of transformation
- Infinite discontinuity in $C_p$

## Second Order Trasformation

- Parent and reactant are same phase.
- NO discontinuous changes in entropy, enthalpy & specific volume.
- NO latent heat of transformation.
- High specific heat at the transition temperature.
- Finite discontinuity in $C_P$ *(NOT infinite)*.

## First order

*E.g.: Melting*

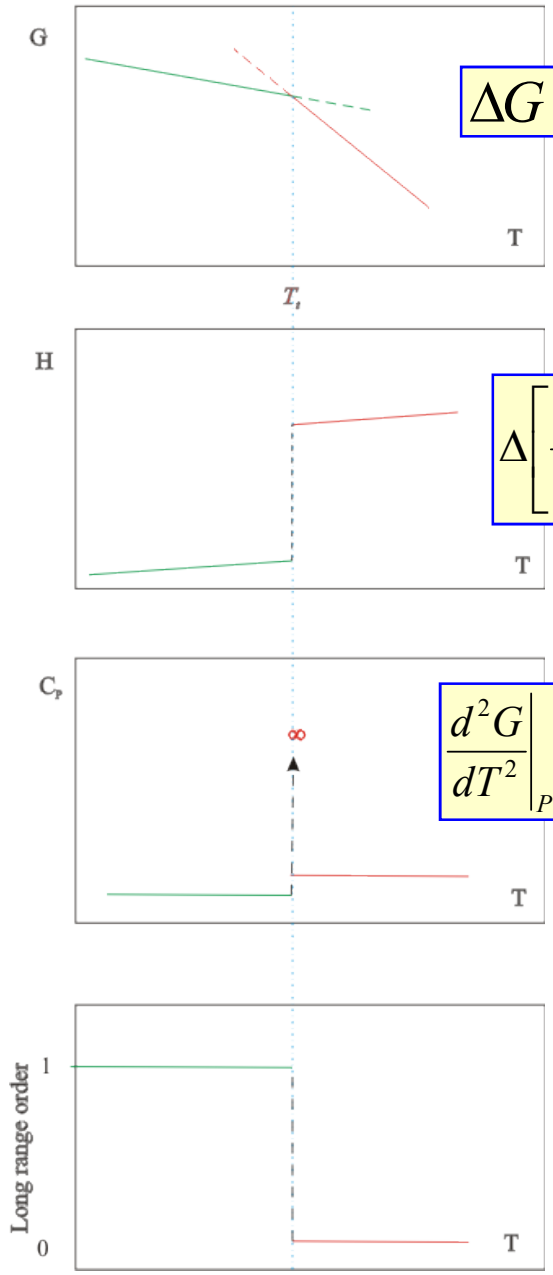


$$\Delta G = 0$$

$$\Delta\left[\frac{\partial^1(\mathrm{G})}{\partial(\mathrm{T})^1}\right]_P = \frac{\Delta H}{T_C} = -\Delta S \neq 0$$

$$\left.\frac{d^2G}{dT^2}\right|_P = -\left.\frac{dS}{dT}\right|_P = \frac{-C_P}{T_C} \rightarrow \infty$$

## Second order

*E.g.: Disordering of β-brass*

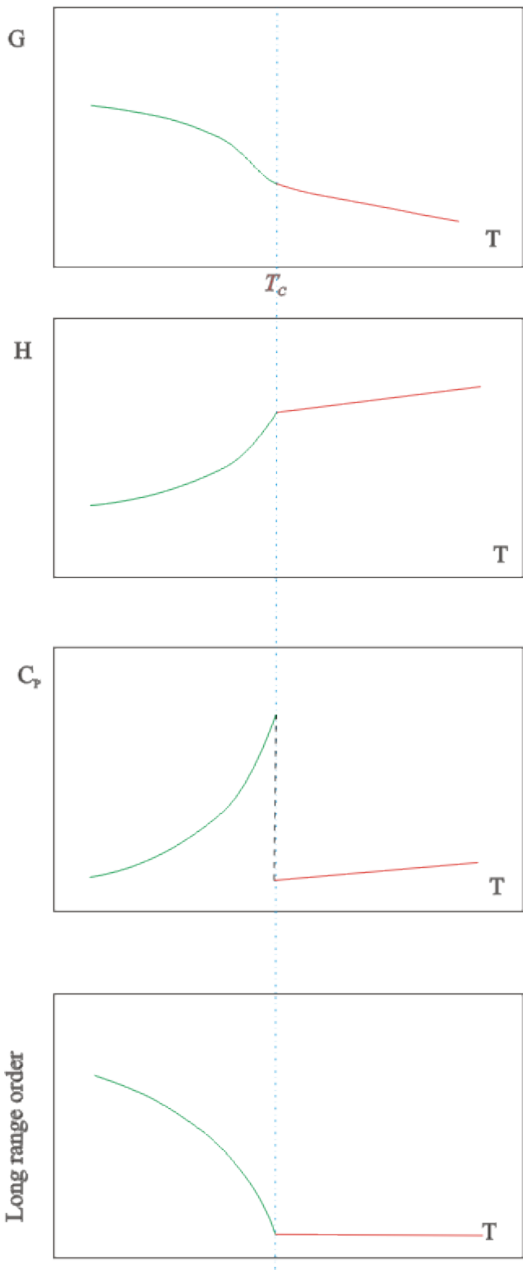

- Formation of ordered superlattice from a disordered solution take place by nucleation and growth.